Volume 41, Number 3, 2015.

Mobility & Vehicle Mechanics

International Journal for Vehicle Mechanics, Engines and Transportation Systems

ISSN 1450 - 5304

UDC 621 + 629(05)=802.0

UNIVERSITY OF KRAGUJEVAC, FACULTY OF ENGINEERING

SERBIAN SOCIETY OF AUTOMOTIVE ENGINEERS

M V M **M**obility **V**ehicle **M**echanics

Editors: Prof. dr ***Jovanka Lukić****; Prof. dr* ***Čedomir Duboka***

For Publisher: Prof. dr Miroslav Živković, dean, University of Kragujevac, Faculty of Engineering

Publishing of this Journal is financially supported from:
Ministry of Education, Science and Technological Development, Republic Serbia

Mobility &		**M**otorna
Vehicle	**Volume 41** **Number 3** **2015.**	**V**ozila i
Mechanics		**M**otori

Mobility & **V**ehicle **M**echanics

Volume 41
Number 3
2015.

Motorna **V**ozila i **M**otori

MOTOR VEHICLES – EDUCATION AND RESEARCH IN SERBIA

Rajko Radonjić[1]*, Aleksandra Janković*

UDC:629.114:[378.225]

ABSTRACT: This paper examines contemporary research and educational problems in automotive industry. In terms of perception and better understanding of the complex interdependence of this issue the block diagram is formed of the man-vehicle interaction in three important observation segments: (1) vehicle development through history, (2) phases of creating the vehicle and its life expectancy, (3) influence of the vehicle on human life. Functions of education and research and their complex interdependence are observed within the mentioned second segment of the block diagram – that is, „phase of the life expectancy of the vehicle“. The following is pointed out: multidisciplinarity of this issue, typical vehicle characteristics considering appropriate species of traffic systems, and transfer of knowledge and technologies in the land-air traffic. Within land transport road traffic is especially in focus and the mentioned current problems in the aspect of research and education. Thereby, special attention is given to the problem of the vehicle control in the complex system of the road traffic that is cybernetic system driver-vehicle-roads-surroundings. This problem is illustrated by the results of the specific researches that signal the complexity of the issue, multidisciplinarity, current measurement equipment need, it is also illustrated by the examination of the contemporary disciplines etc. Basing on the general situation and trends in the world and the current problems in Serbia, as well as the approach in this paper, it is possible to critically analyze the past and the current condition in the subject areas with more realistic designs of the future condition and taking the necessary measures in order to improve it.

KEY WORDS: motor vehicles, higher education, research, Serbia

MOTORNA VOZILA – EDUKACIJA I ISTRAŽIVANJE U SRBIJI

REZIME: Ovaj rad se bavi proučavanjem savremenih istraživanja i obrazovnih problema u automobilskoj industriji. Po pitanju opažanja i boljeg razumevanja složene međuzavisnosti ovog pitanja, formira se blok dijagram interakcije čovek-vozilo u tri važna segmenta zapažanja: (1) razvoj vozila kroz istoriju, (2) faza stvaranja vozila i njegov vek trajanja, (3) uticaj vozila na ljudski život. Funkcije obrazovanja i istraživanja i njihove kompleksne međuzavisnosti se posmatraju u okviru navedenog drugog segmenta blok dijagrama – da je, “faza od životnog veka vozila”. Istaknuto je sledeće: multidisciplinarnost ovog pitanja, tipične karakteristike vozila s obzirom na odgovarajuće vrste saobraćajnih nezgoda i transfer znanja i tehnologija su u kopneno-vazdušnom saobraćaju. U okviru kopnenog saobraćaja drumski saobraćaj je posebno u centru pažnje sa pomenutim aktuelnim problemima u pogledu istraživanja i obrazovanja. Pri tome, posebna pažnja je posvećena problemu kontrole vozila u složenom sistemu drumskog saobraćaja koji je kibernetski sistem za vozač-vozilo-put-okolina. Ovaj problem je ilustrovan rezultatima specifičnih istraživanja koja ističu složenosti ovog pitanja, multidisciplinarnost, potrebu za mernom opremom, takođe je ilustrovano ispitivanje savremenih disciplina itd. Na osnovu opšte situacije i trendova u svetu i trenutnih problema u Srbiji, kao pristupu ovom radu, moguće je kritički

[1] *Received: September 2014, Accepted October 2014, Available on line: May 2015*

analizirati prošlo i sadašnje stanje u oblastima sa realnijim dizajnom budućeg stanja i preduzimanje neophodnih mera kako bi došlo do unapređenja.

KLJUČNE REČI: motorno vozilo, visoko obrazovanje, istraživanje, Srbija

MOTOR VEHICLES – EDUCATION AND RESEARCH IN SERBIA

Rajko Radonjić [1], Aleksandra Janković[2]

UDC: 629.114:[378.225]

INTRODUCTION

Motor vehicle, in the aspect of science and research, and also of profession, is a multidisciplinary object. It represents ideal training ground for implementation of the new scientific discoveries and technical achievements of the material field (first of all composites for auto body parts and even vital elements of the machinery group), of electronics and automatics (which find the widest application through automatisation of the control process and control), and of human disciplines such as ergonomy and professional occupational medicine.

In terms of the scope of production it can be the object of mass production, retail or individual production of the various types of vehicles and vehicles for various purposes, passenger vehicles (sport vehicles, family vehicles, public transportation vehicles), goods vehicles (light, heavy, and goods vehicles for special purposes).Each of these products demands specific knowledge.

- Education in developing and achieving global competitiveness, as well as positioning in the world's leading teams,or,
- Education in licensing the production of passenger/ goods vehicles programme or
- Education in producing and maintaining agricultural vehicles and working machinery, trailer vehicles?

Specialized, or General Mechanical Engineering?

Mechanical or Industrial or Traffic Engineering?

Strategic issue! In order not to turn into rhetorical question, it is necessary to wisely adjust the development of the whole society with education, considering surroundings and scientific, political and economic trends. Which with what? Should technical intelligence be directed so that education adjusts the needs and possibilities of economy or should economy be directed towards educational trends? Which came first, the chicken or the egg? The answer is neither, but the dynamic interaction of education, development and production should be provided.

[1] *Rajko Radonjić, Full professor, Faculty of Engineering, University of Kragujevac, Sestre Janjić 6, Kragujevac, rradonjic@kg.ac.rs,*
[2]*Aleksandra Janković,Full professor, Faculty of Engineering, University of Kragujevac, Sestre Janjić 6, Kragujevac,alex@kg.ac.rs*

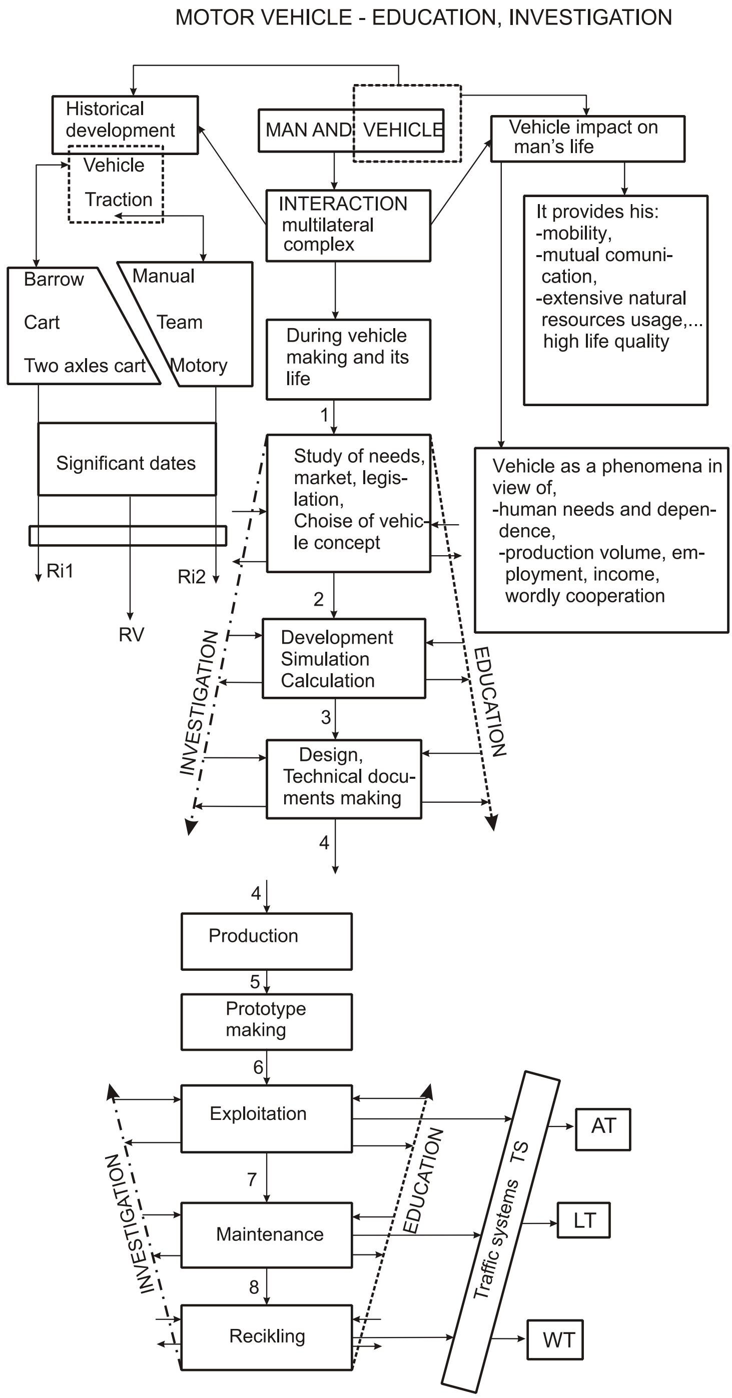

Figure 1 Connection between man and vehicles

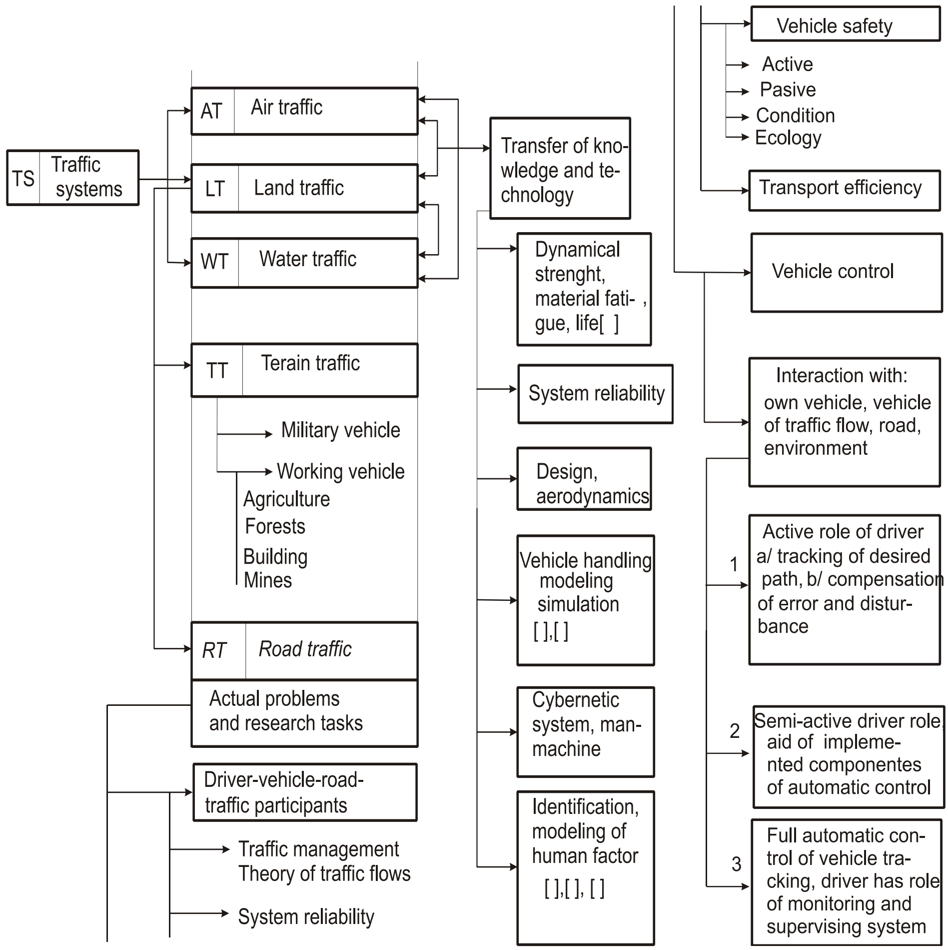

Figure 2 Connection between traffic, man and vehicles (left) and actual investigation (right)

THE SITUATION IN SERBIA

Strategic plan to industrialize SFRY initialized the development of the motor industry in Serbia and in the region of Yugoslavia. Thereby they particularly insisted that the mainstream, development and subcontractors expand throughout all the country and this mainly had political, rarely economic background. Production machineries were built and education of engineers was needed. Industry demanded technically educated personnel, starting from the production workers, through machinery administrators – technicians and engineers, and all the way to the creative workers -constructors, technologists, analysts and experimental engineers. Thus technical schools of various levels of education arose, secondary schools, academies and faculties.

Faculty of Mechanical Engineering in Kragujevac was founded out of need to educate mechanical engineers that would become part of the former giant Factory „Crvena zastava“. It was based on two directions, Production engineering and Motor vehicles. Educational platform of the motor vehicles, as multidisciplinary and interdisciplinary objects of research and production, expanded and changed. Development and education intertwined seeking support one from another. By this extracting of the motor vehicle's fundament from the rest of the production machinery, including automobile production, the development of the motor vehicles was stressed in our country. Disciplines fundamental in the vehicle's development were studied, first of all contemporary measurement methods and examination methodologies, computational mechanics and mechatronics, dynamics and thermodynamics.

For fifty years was done much. Some of the results are shown in the following figures.

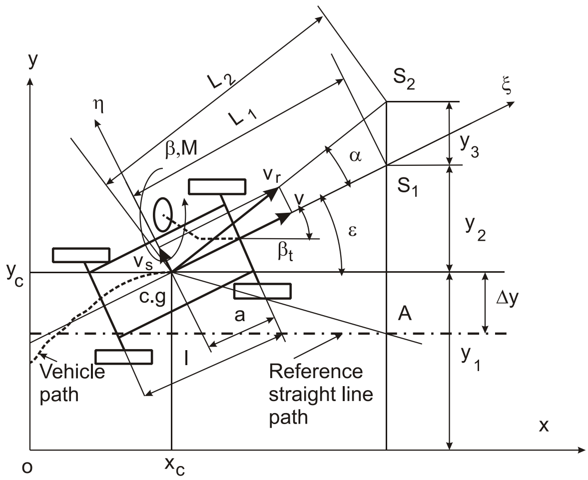

$$\Delta Y = \Delta y + y_2 + y_3 \cong \Delta y + L_1\varepsilon + L_2\alpha$$

Figure 3 Geometric presentation of vehicle-visual field interaction on straight line path

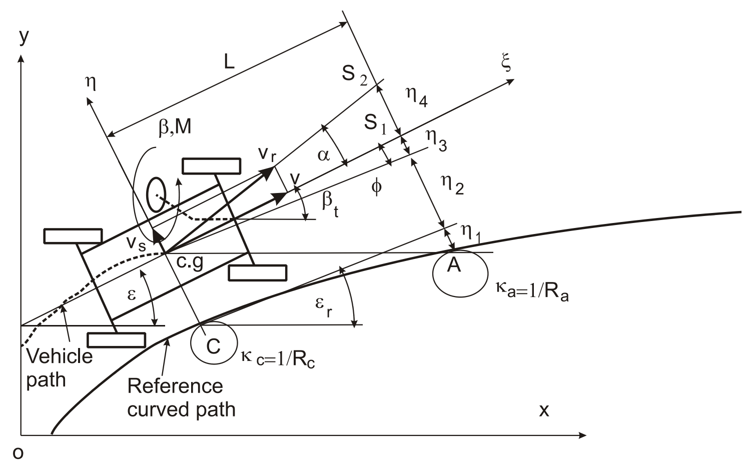

Figure 4 Geometric presentation of vehicle-visual field interaction on curved path

Geometric diagrams of a vehicle model following a reference straight line path and a reference curved path, to investigation in this paper, are given in Figure 3, 4, respectively.

Geometric diagram of vehicle model following a reference curved path, in Figure 4, is a generalization of previous model given in Figure 3.

Advanced lateral deviation of vehicle as sum $\eta_1 + \eta_2 + \eta_3 + \eta_4$, is oriented perpendicular on tangent of curved reference path in point C, near of vehicle centre gravity c.g, with adequate segments, $\eta_2 \rightarrow \Delta y$, $\eta_3 \rightarrow y_2$, $\eta_4 \rightarrow y_3$, and unique sight point distance L.

Segment η_1, is part of perceived deviation as coordinate of aim point A, from tangent on curved path in point C.

In the compensatory control mode, based on the previewed lateral deviation, command input from curved path is only one cue, the aim point A. On the other hand, in the anticipatory control mode, command input from reference curved path is curve segment finite length which driver estimates and uses as visual information.

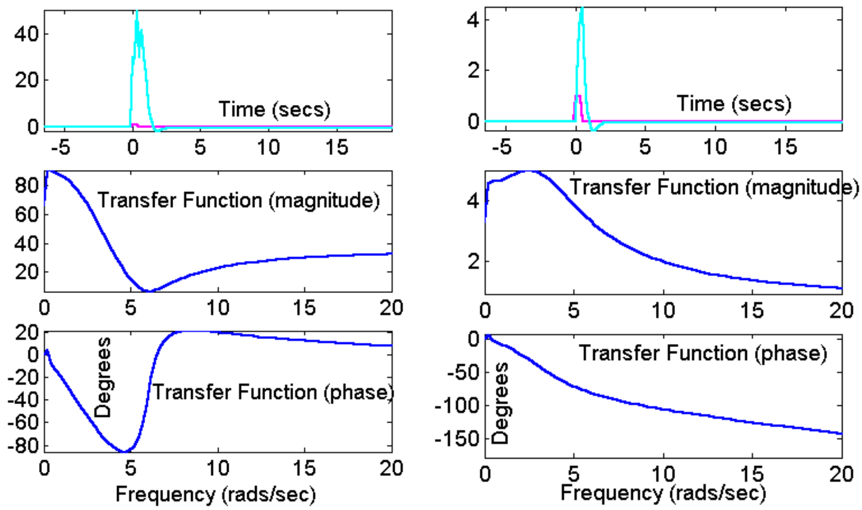

Figure 5 Vehicle transfer function, input – steering wheel angle, output: a/ lateral acceleration,b/ yaw velocity. Longitudinal velocity, 20m/s

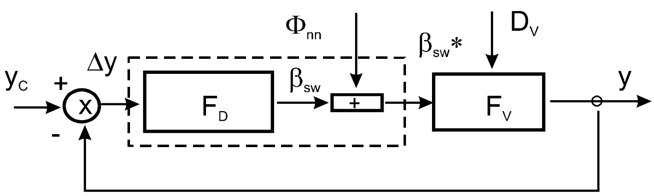

Figure 6 Block diagram of single-loop driver/vehicle system.

The rational of driver equalization can be approximated by ″ crossover model ″, according to Figure 6:

$$F_D F_V = \omega_c \frac{e^{-j\omega\tau_e}}{j\omega} \qquad (1)$$

where, τ_e– includes the neuromuscular time constant, T_N, as well as,τ.

Generally, drivers use multiple information as input for controlling the vehicle. Good multi-loop system structures are those which no require the driver equalization, for example, only gain plus time delay in each of the loops. But driver dynamics as a multi-input system is often approximated by equivalent a single loop system. In the study [12], driver dynamics is described by equivalent closed – loop system which comprising vehicle lateral position and yaw angle feedback loops from corresponding multiple loop. This model is useful to examine the vehicle with 2WS steering system which shows a close correlation between its yaw angle and lateral position response, Figure 7.

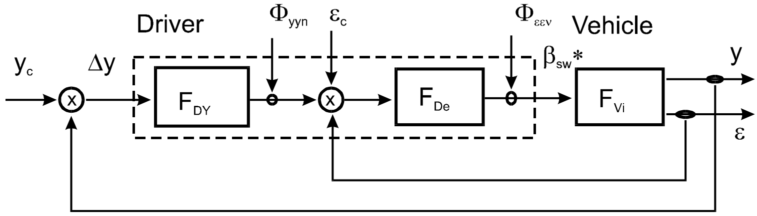

Figure 7 Block diagram a comprising multi-loop driver/vehicle system

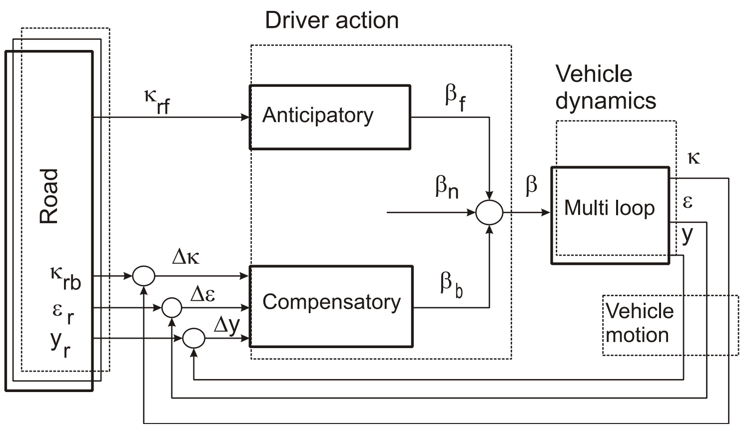

Figure 8 Block diagram of road-driver-vehicle control system

Driver can improve the system control performance by using derived path command information in visual field and operating in anticipatory mode. That is, driver can perform the steering task hierarchically into two levels, guidance and stabilization, [15], [16]. In the case of driving into a curve, driver perceives desired path curvature and responds to it an anticipatory open – loop control mode with a part of total necessary steering wheel angle. Based on the perceived path error in closed – loop compensatory mode the driver generates a correcting steering wheel angle, Fig. 4, 8, 9.

By forming driver model based on the concept – vehicle lateral deviation advanced in time, it assumes that driver operates on an estimated or projected lateral deviation error of vehicle centre gravity, Δy, Figure 3, 4. The perceptual preview time, as relation driver look – ahead distance and vehicle forward velocity results in a pure lead equalization term in effective vehicle dynamics.

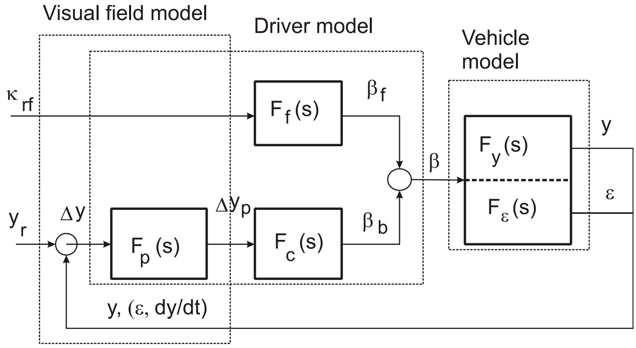

Figure 9 Model of visual field-driver-vehicle control system

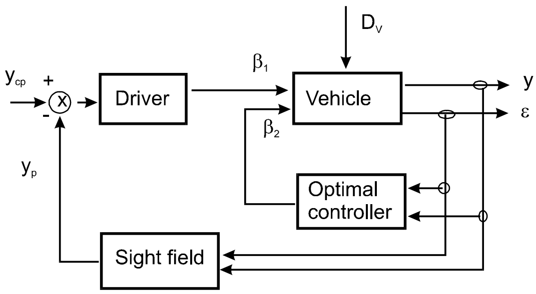

Figure 10 Block diagram of the driver/optimal controller/vehicle system

The vehicle do not possesses own stability of the lateral displacement in relation to desired path. To study the vehicle lateral stability the driver or other controller, which perform his function, must be included. In this paper, the behaviour driver/ (controller) /vehicle system and its components is considered according to block diagram in Figure 10. The following combination are examined: a) vehicle in the open loop with defined steering wheel position, b) vehicle in the closed loop steered by driver, c) vehicle in the closed loop steered by optimal controller, d) vehicle in the closed loop steered by driver and optimal controller.

2-axis Optical
CORREVIT®
Speed & Distance for Slip-Free Measurement of Longitudinal and Transversal Dynamics
& Slip Angle Sensors

a)


b)

Figure 11 MSW/S - Measurement Steering Wheel for non-contact measurement of steering speed and angle

a) 2 – axis Optical CORREVIT Sensors (Speed, Distance, Slip Angle Measurement)

b) Sensors for non-contact measurement of steering wheel speed and angle


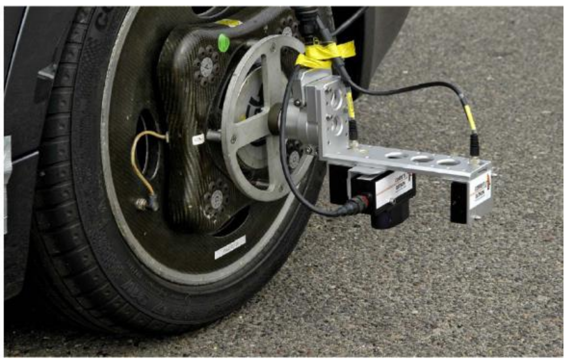

a) *b)*

c)

Figure 12 a)dynamic camber mesurement, b) wheel force transducer and dynamic camber measurement, c) Contidrom Proving Ground [21]

a)

b)

c)

d)

e)

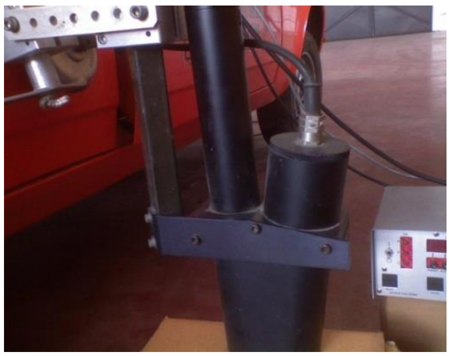

f)


g)

h)


i)

j)


k)

l)

Figure 13 Sensors for Motor Vehicle Measurement: a), c) steering wheel speed, angle and torque, b) brake pressure HBM, d), e), f), h), i), j), k), l), vehicle lateral and longitudinal velocity Leitz – Correvit,L - , Q- Sensors, d), g) wheel angular velocity, own design.

(Motor Vehicle Laboratory, Faculty of Mechanical Engineering Kragujevac, MVL/FMEK)

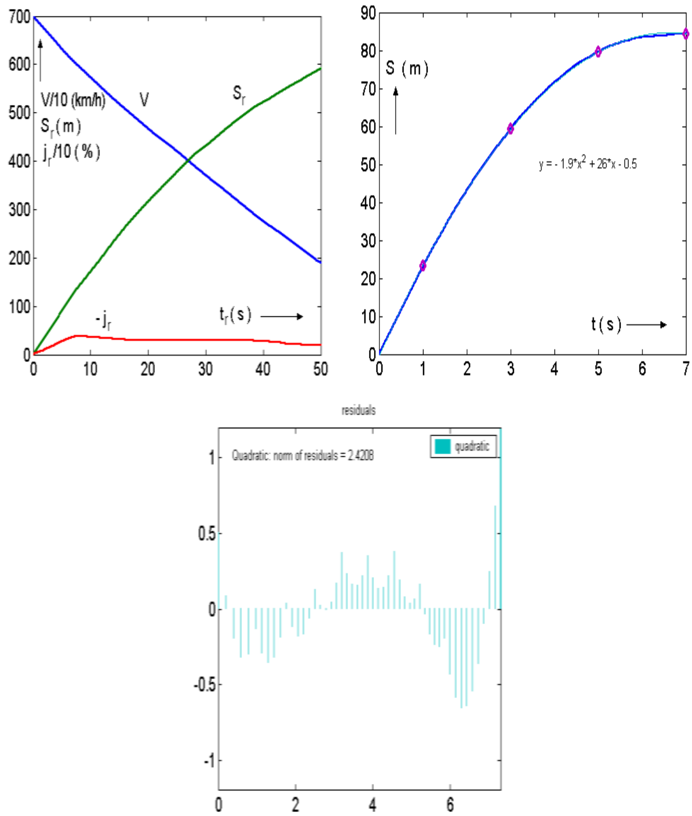

Figure 14 Experimental results of the vehicle traction and braking performance of MVL/FMEK

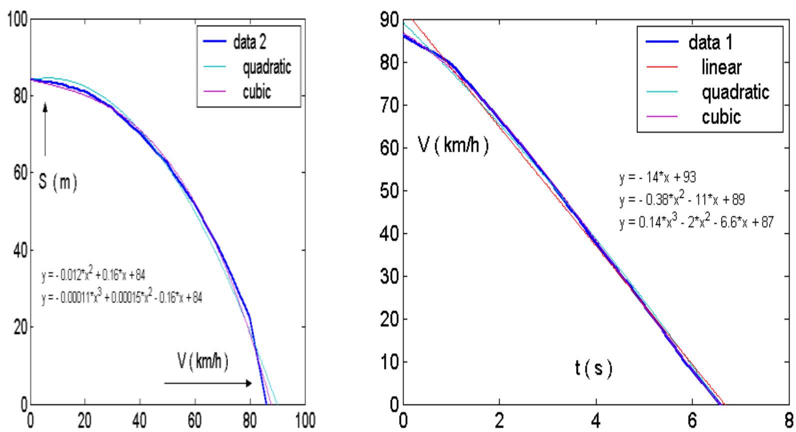

Figure 15 Experimental results of the vehicle traction and braking performance of MVL/FMEK

a) b)

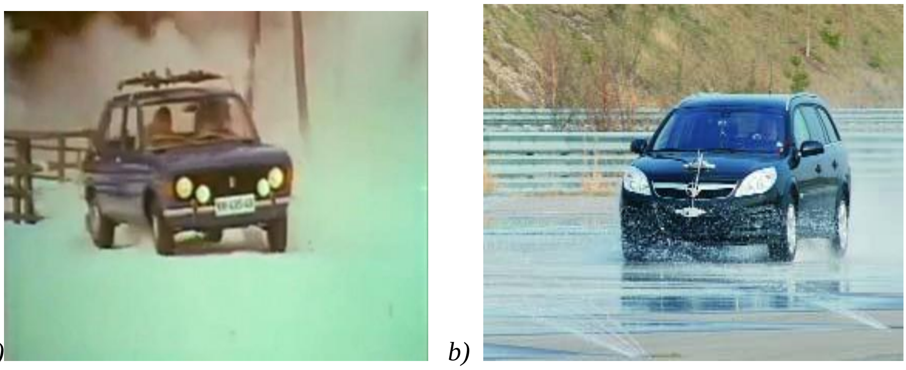

Figure 16 Different condition to vehicle testing, [22]

The first personnel that were supposed to carry out the production burden were the mechanical engineers of the Department of the Faculty of Mechanical Engineering of Belgrade University, the 1960. generation. That generation could choose between the production engineering or motor vehicles in accordance with the needs of the industry in Kragujevac in those days. Besides Belgrade University, Universities of Novi Sad and Niš also existed but motor vehicles as an individual discipline were not recognizable. Capital cities of the Republics of the former Yugoslavia and Belgrade were leading in the development of the field of engines and motor vehicles, and Kragujevac was the first city from the inland that started the strong development of the integrated industry and education.

Automobile factory that developed as expansion of the already existing military technical industry, was based in Kragujevac but it had subcontractors all over Serbia and in other republics of Yugoslavia. As a huge novelty and support to the construction, calculations were made as well as experimental researches. These two areas were precisely the germ of the development of motor vehicles that sustained in Serbia mostly through modelling and aggregate examination.

Our faculty had foreign support during the 1970s through Humboldt, Fulbright and other scholarships for our PhD students who worked their dissertation mostly in Germany and America, but also in other European countries. After that they would come back to Serbia and bring their knowledge, educational spirit, and organizations of the most developed countries here to this very ground. Besides this personnel support, and creating of the human resources, we also received help in terms of the research equipment, thus unique contemporary measurement equipment from the West Germany (analogue computer and numerous analogue measurement instruments), as a development and cooperation support in the area of the motor vehicles, came to this very faculty.

After the year of 2000. a lot of donation were made for contemporary, digital research equipment, this was the support of the developed countries in order to surpass the abyss after the breakup of Yugoslavia and our perennial isolation, but the supplied equipment was utilized and oriented in a different way, because of the significantly different social circumstances. Very modest mobility donations were intended for the researches and teachers of the motor vehicles area, the area where great progress was made in the world, which further degraded higher education of this field after the motor and vehicle industry breakup.

This symposium is one of the branches out of the trunk of the synthesised scientific discipline “motor vehicles and engines”. How long will it be thematically sustainable considering the fact that the economy support is getting weaker and weaker? Will it become overview of the world situation or will it succumb to the trend of the industrial and traffic engineering development?

Universities, higher education and secondary schools in the motor vehicle area suffered great stagnation or even extinction as a result of social changes and economy situation. Transformation was needed, but it was implemented without any strategy, and when a strategy was adopted, it was not consistently applied, it was warped according to the personality strength or according to the inertia to sustain the existing with surface changes, the result was quite a chaos in higher education.

The reason for the transformation of the development of engineering into production engineering lies in basic need to withstand competition on the market of the higher education. After the isolation period, destruction and closeout of our economy we did not have a training ground for our students nor did they have a future in terms of the employment. We welcomed FIAT with open arms, a company that came to our country for its own profit and that requires production organisation, logistics and automatics, with English language knowledge by default. This is the reason why many our experienced engineers did not manage to find their place in this completely new surroundings. They have not been adequately prepared for this kind of technology and production organization, and it was too late to make efforts to master the new knowledge and skills. They forgot that intellectuals have to be perpetual students, in order to remain a competitor in the global market match. Besides, for the new process and volume of the production fewer people are needed, so the number of students and curriculum should have been adjusted to the innovated motor vehicle industry. How?

Present model of study, which continuously promotes the so called mobile students, allows that students go to higher levels of study in the developed countries, thanks to the adjusted and accredited programmes of study or to the research projects. This departure is mostly in one way, for the time being, that is from the parent country to the foreign countries. Are the causes of the one way traffic found only in the conditions for the research or in the living standard or in our misgiving that we will have to necessarily change ourselves by creating environment that will bring the new rules and new standards and habits. Isn't our inertia and a dose of self-love the reason for our slow integration in the developed world that frightens us a bit. If inertia and the fear from the ones that are better settle into higher education institutions, then the higher education and the whole society go downhill. If the ambition is heating up vanity and becomes so powerful that it conquers the space that should be conquered by the breadth of spirit, then the research turns into plagiarism or the personal success is shared as an apparent team success and the academic community is rushing to become "emperor in his new suit". What we never succeeded to valorise through the last reform of the higher education, and which is estimated worldwide, is the contribution of the intellectuals to the society. Did the insisting on the quantity of the printed papers and the number of students, rather than their spontaneous and natural expansion, give positive or negative effects the time will show.

Otherwise, the broader platform was created over time in mechanical engineering through interaction of classic, original engineering and electrical engineering with electronics, first of all, but also organizational sciences, human and bio-technical sciences, standardisation and technical law, so the mechanical engineers always had an open network of trails through their professional career. That network had knots and narrow paths, precipitous paths and wide, flat paths in its structure, so everybody could choose and change the road according to their abilities and affinities, there is a saying that "mechanical engineers know everything".

HOW TO CONTINUE?

How should the education and training for motor vehicles research be conceived? Did the development of the new disciplines significantly influence on divergence in mechanical engineering education, from the 30 year ago training, or the community orientation to its own production and import industry had the greater influence on educational changes. The answer is both. The development of the new scientific disciplines associated with IT “dragged” one part of the engineers to those new domains, which is a positive thing, while the destruction of the production resources and illegal trade caused to develop a great number of unaccredited business academies, that had a bad influence on the whole higher education system. It may not seem to be like that right away but rapid graduation and possibility to continue education caused the average level of the faculty students to descend. Economy destruction definitely caused the decline of the criteria on technical colleges because of the lack of the rapid employment motif, and getting the mechanical engineer for motor vehicles diploma was not easy a task so the number and the quality of the interested graduates for this kind of study decreased.

Therefore the solution for quality technical education lies in interaction with industry, which is now achieved through clusters, where colleges are increasingly included. This is not a new idea but promotion of region development and technical progress of IT networks creates favourable climate for this kind of cooperation. Economy-research-higher education is a triangle which is stable in every social system and this bracing gives results, whether it is achieved in region or through international institutional cooperation.

Significant participation of scientific research in higher education and a high level of permeating of these two domains raise university education above all the other heigher education. However, complete equalization of higher education and scientific research, degrades the very education because this imposes a match in which education loses tradition component. The educational and innovative component should undoubtedly be in strong correlation concerning the university education. What is the good measurement between these two components? It changes depending on the level of development and the gradients of scientific development in a society. Sometimes or more precisely somewhere their own research is dominant and somewhere the researches are interpreted and taken from the developed countries and education is dominant. Our country was not lucky enough, the motor industry and vehicle industry did not develop as they started to develop during the 1970s and the 1980s, but the ascend was cut down during the 1990s, so the researches stagnated and apart from some exceptions we had to follow what happens in the area of the motor vehicles in foreign countries and reproduce this to our students. Our engineers lost their job and most of them never recovered professionally.

Globalisation that imposes high speed changes, emphasizes competition, cruel match between the most prestigious who take as their partners the most capable ones who are able to follow them and contribute to their success, causes vanishment of those who are not capable to be the part of this composition, which has its tracks through projects such as Horizont 2020, and its projection reflects through highly specialized clusters of the developed. Social circumstances, region development, circumstances and political climate imposes business economy that especially reflects on university education in techniques and economy. Motor vehicles completely depend on these two areas.

Europe accepted the new model of graded studies and huge diversifications in the curriculums, educating the new profiles including interdisciplinarity and also often multidisciplinarity. On the other hand, the narrow domain is created for the most talented, the so called excellent scientific research field, the excellent centres are created, research and development centres and university centres that raised the relevant platform of knowledge in a unique synergy. This platform has clearly defined scientific areas that are priority to develop till the year of 2020 and traffic and vehicles are among them, but in a different dimension and with the aim of different knowledge outcome. The world of technique sharply polarized, high technologies and researches in the field of micro, nano and opto technologies are on one side, and on the other side are highly organized production systems which function as black boxes and for which good logistics, top organization and communication should be provided, the rest of it regulated someone who knows it. Where are Serbian higher technical schools and technical faculties in the whole story?

CONCLUSIONS

At this point it is certain that the broader space is being created for the mobility of the teachers and students, that international cooperation and compatibility of the curriculum are forced, which is a positive thing, however our own home is being neglected in terms of national economy development. Total acceptance of everything that grows on somebody else's field causes our becoming humble guests in our own house. Greater commitment to the national interest will not shut the door on the world. On the contrary, our recognizable identity in education and a level of usage of that knowledge to raise the living standard will be reflection of the higher education success. .

ACKNOWLEDGMENTS

We are grateful to Tijana Biberdžić for the translation of this article.

REFERENCES

[1] Appel H., Breuer B.,Essers U.,Helling J., Willumeit H-P. UNI – CAR Der Forschungs – Personenwagen der Hochschularbeitsgemeinschaft . (UNI – CAR – The Research Car of the University Team). ATZ – Automobiltechnische Zeitschrift 84(1982)3.

[2] Appel H., Meissner, T. Grundlagen der Kraftfahrzeugtechnik II. Umdruck zur Vorlesung, TU Berlin, Institut fur Fahrzeugtechnik, Berlin 1998.

[3] Bohm F. Uber die Fahrrichtungstabilitat und die Seitenwind empfindlichkeit des Kraftwagens bei Geradeaus – Fahrt, ATZ , 1961.

[4] Chenchanna P. Untersuchungen uber des Lenkverhalten von Fahrzeugen bei verschidenen Modellen fur Fahrer. Dissertation, TU Berlin, 1966.Reference 4,

[5] Fiala E. Lenken von Kraftfahrzeugen als kybernetische Aufgabe. ATZ 1966.

[6] Isermann R. Processidentification. Springer Verlag, 1974.

[7] Isermann R. Fahrdynamik – Regelung. Modellbildung, Fahrerassistenzsysteme, Mechatronik, 2006.

[8] Jaksch F. Driver – Vehicle interaction with respect to steering controllability. Volvo Car Corporation, Sweden, SAE 790740.

[9] Janković S. Zapisi o Zastavi. Zastava Kragujevac, 1993.

[10] Janković A. Dinamika automobila. Kragujevac 2008.

[11] Jovanović S. Sto godina automobila u Srbiji. Beogradski sajam, 2003.

[12] McRuer D, Krendel E. The human operator as a servo – system element, Journal of Franklin institute, 1959.

[13] Mašinski fakultet u Kragujevcu, Monografija povodom 35. godina studija mašinstva, Mašinski fakultet, 1995.

[14] Radonjić D. Razvoj nastave i obrazovanje kadra na Mašinskom fakultetu u Kragujevcu. Drugi skup katedri za motore i motorske indusatrije, str 175 – 179, Neograd 1994.

[15] Radonjić R. Identifikacija dinamičkih karakteristika motornih vozila. Monografija, Mašinski fakultet Kragujevac, 1995.

[16] Radonjić R., Janković A., Aleksandrović B., Radonjić D. Modeling of driver behaviour. International Congress Motor Vehicles and Motors, MVM 2012 – 002, pp. 401 – 410. Kragujevac

[17] Rankin W., Allen J. Use maintenance error decision aid to enhance safety and reliability and reduce costs in the commercial aviation industry. Boeing Group, Seattle, 1995.

[18] Simić D. Beitrag zur Optimirung der Schwingungseigenschaften des Fahrzeuges – Phisiologische Grundlagen des Schwingungskomforts. Dissertation TU Berlin, D83 1970.

[19] Todorović J. Tehnika motornih vozila na Mašinskom fakultetu u Beogradu. Saopštenja Mašinskog fakulteta u Beogradu 1982, str 46 – 52.

[20] Todorović J. Ispitivanje motornih vozila. ;Mašinski fakultet u Beogradu, 1979.

[21] Weimert K., Barz D. An example for Camber and Wheel Force Measurements for the Generation of Test Stand Data and Validation Purpose. www. Corrsys – Datron.com

[22] www. Corrsys – Datron. com.

DEVELOPMENT OF CONTINUOUSLY VARIABLE INTAKE MANIFOLD FOR FORMULA STUDENT RACING ENGINE

Predrag Mrdja [1], Vladimir Petrović, Stefan Đinic, Marko Kitanović

UDC: 62.843.4:[519.673]

ABSTRACT: After several years of research and development of Formula Student's air mass flow restricted racing engine at the Internal Combustion Engines Department of the Faculty of Mechanical Engineering, University of Belgrade, the design process of a new intake manifold for the 2014 competition season was set off. Through several seasons, the intake manifolds of the YAMAHA YZF-R6 high performance engine evolved from a dual volume, into a single volume concept and finally to the continuously variable intake manifold (CVIM) design. Comparative analysis of data obtained during in-laboratory engine testing and data logged from ECU during the races gave some guidelines in the design of CVIM. The main goal of this research is increasing the number of engine operating points with resonant supercharging. The Ricardo WAVE engine mathematical model is improved and particular attention is dedicated to the approximation of the adopted CVIM concept using Helmholtz Resonance Theory. This paper describes the correlation between optimal intake runner length and manifold volume over engine speed at wide open throttle as well as their influence on volumetric efficiency and engine effective parameters.

KEY WORDS: engine testing, variable intake manifold, optimization, resonant supercharging, Formula Student

RAZVOJ KONTINUALNO PROMENLJIVE USISNE GRANE ZA MOTOR FORMULE STUDENT

REZIME: Nakon nekoliko godina istraživanja i razvijanja protoka vazdušne mase Formule student ograničenog trkačkog motora na katedri Motora sa unutrašnjim sagorevanjem Mašinskog fakulteta, Univerziteta u Beogradu, proces projektovanja nove usisne grane za sezonu 2014 je počeo. Kroz nekoliko sezona, usisna grana YAMAHA-e YZF-R6 motora visokih performansi je evoluirala od koncepta dvostruke zapremine u koncept jedne zapremine i konačno do koncepta (CVIM) kontinualno promenljive usisne grane. Uporedna analiza podataka dobijenih tokom laboratorijskih ispitivanja motora i podataka očitanih od ECU tokom trke daje neke smernice u dizajnu CVIM. Glavni cilj ovog istraživanja je povećanje broja radnih tačaka motora sa rezonantnim predpunjenjem. Rikardov WAVW matematički model je unapređen i posebna pažnja je posvećena aproksimaciji usvojenog CVIM koncepta primenom Helmholzove rezonantne teorije. Ovaj rad opisuje vezu između optimalne dužine usisa i zapremine usisne grane zavisno od broja obrtaja motora sa potpuno otvorenim leptirom, kao i njihov uticaj na zapreminsku efikasnost i efektivne parametare motora.

KLJUČNE REČI: ispitivanje motora, promenljiva usisna grana, optimizacija, zvučno predpunjenje, Formula student

Intentionally blank

DEVELOPMENT OF CONTINUOUSLY VARIABLE INTAKE MANIFOLD FOR FORMULA STUDENT RACING ENGINE

Predrag Mrdja[1], Vladimir Petrović[2], Stefan Đinic[3], Marko Kitanović[4]

UDC:62.843.4:[519.673]

INTRODUCTION

Formula Student (FS) is a global student engineering competition, whose rules are prescribed by the Society of Automotive Engineers (Formula SAE)[1] and individual amendments to the rules and by the other competition organizers (Formula ATA [2], FSA [3], FSG [4], FSH [5], etc.). Students at different study levels, B.Sc., M.Sc. and Ph.D., at the Internal Combustion Engines Department (ICED), Faculty of Mechanical Engineering, University of Belgrade are involved in this contest taking a part in the development, production and testing of power train and electronic systems of the racing vehicle. The main goal of this paper is presenting results of there search dedicated to continuously variable geometry intake manifold (CVIM), engine test results and providing guidelines for the design process.

The applied technical solutions that will be used in the 2014 competition season are obtained taking into account the experience gained in previous years of development and research aiming at performance increases in terms of engine effective torque over certain RPM. Using Ricardo WAVE simulation environment, engine mathematical model is constantly improved through an iterative process of model validation and calibration coupled with in-house developed MATLAB post-processing and decision-making codes.

The design process of complex engine's systems such as CVIM is divided into several stages. It is very important to use high-quality data obtained during in-laboratory engine testing based on the predefined engine test plan in order to achieve the best possible engine mathematical model matching. Also, the availability of the test equipment, "know how" resources, production technology and affordable budget are key features. Considerable attention is paid to logging setup and to the analysis of the data logged during the races. In this manner, important conclusions about the entire power train system are drawn. Additionally, this paper will briefly present theoretical bases of resonant supercharging, CVIM concept review in the way of actuation and part of the simulation results which are used for control look-up tables.

[1]*Predrag Mrđa, M.Sc., Teaching Assistant, Internal Combustion Engines Department, Faculty of Mechanical Engineering, University of Belgrade, Kraljice Marije 16, 11120 Belgrade 35, Serbia, pmrdja@mas.bg.ac.rs*
[2]*Vladimir Petrović, B.Sc., Research Assistant, Internal Combustion Engines Department, Faculty of Mechanical Engineering, University of Belgrade, Kraljice Marije 16, 11120 Belgrade 35, Serbia, apoc@gmail.com*
[3]*Stefan Đinić, B.Sc., Research Assistant, Internal Combustion Engines Department, Faculty of Mechanical Engineering, University of Belgrade, Kraljice Marije 16, 11120 Belgrade 35, Serbia, djiki21@yahoo.com*
[4]*Marko Kitanovic, M.Sc., Teaching Assistant, Internal Combustion Engines Department, Faculty of Mechanical Engineering, University of Belgrade, Kraljice Marije 16, 11120 Belgrade 35, Serbia, mkitanovic@mas.bg.ac.rs*

ENGINE TESTING

For the purpose of the Engine Control Unit (ECU)[6]optimal control maps determination, the testing of naturally aspirated air mass flow restricted Yamaha YZF-R6 engine was performed during the competition seasons of 2012 and 2013. The idea of CVIM implementation to the Yamaha's power unit is intended for the 2014 season and all calculations, assumptions and results obtained during testing were used in this sense. The basic characteristics of the test object are given in the Table 1.

Engine intake must be equipped with a 20 mm diameter restrictor section which is in accordance with the FS competition rules. The engine was coupled to a Schenck W130 Eddy current dynamometer with a corresponding control module that enables required stable operating regime.

Table 1 Engine and ECU specifications

Engine	YAMAHA YZF-R6, four stroke, spark ignition, in-line four cylinder, naturally aspirated, water cooled	
Ignition order	1-2-4-3	
Bore	67 mm	
Stroke	42.5 mm	
Compression ratio	13.1 [-]	
Valves per cylinder	4	
Restrictor diameter	20 mm	
Competition Season	2013	2014
Runner length (RL)	Optional 180 mm, 210 mm and 240 mm	Continuously Variable 164 mm to 260 mm
Intake plenum volume (V)	Fixed 3.4 lit	Continuously Variable 4.3 lit to 3.7 lit
Engine Control Unit (ECU)	DTA S60 PRO	DTA S80 PRO
ECU interface software	DTASwin 63.10	DTASwin 67.00
Injection	Sequential	
Ignition	Sequential	
Lambda sensor	Wide band	
Communication	Serial, CAN	

Because of the growing idea to develop a CVIM system, during the design process of the in take manifold for the 2013 competition seasonand during in-laboratory engine testing, it was very important to collect as much data as possible with different configurations of the intake manifold. Regarding this, the optimization of the advance timing and the injection duration was conducted with three different runner lengths: 180 mm, 210mm and 240mm (not including the length of intake line within the cylinder head) and constant plenum volume of 3 liters. The engine operating regimes on which the experiments were conducted are very similar to the ones explained in the previous studies of the author [7, 8].Because of the inability to avoid detonation at high load and low RPM regimes, and nearly zero value of effective torque at high RPM and no load regimes, some values of control maps are determined based on previous experience.

Data acquisition

All sensor readings were set in time domain to simultaneous 1k sample per second. Readings from stock engine sensors, which were used as ECU inputs, and some output (control) parameters were available on the high speed ECU's CAN data stream (total of 24 channels within 6 messages). Established CAN communication enabled data-flow of all available ECU's data to the acquisition system based on the National Instruments (NI) PXI hardware with maximum frequency of 50Hz. Serial communication between the ECU and PC allows real-time adjustment of engine control parameters (advance timing, injection duration and others) and monitoring of sensor readings (engine speed, throttle position, lambda sensor reading, intake air, coolant and oil temperature, intake air and oil pressure, manifold absolute pressure, battery voltage and others). Besides listed engine parameters, by using an open ECU interface, it was possible to adjust PID coefficients of all closed loop corrections and additional look-up tables (engine start fueling, idling, temperature compensations, etc.).The engine test stand was equipped with some inevitable sensors, which provided monitoring of the parameters, like effective brake torque, transmission output shaft angular speed, exhaust gas temperature, intake air temperature, coolant pressure and temperatures, oil pressure and temperatures and A/F ratio. The acquisition of the analog signals was improved by utilizingin-house developed analog input multi-channel amplifier modules [9]. Along with the data acquisition, the NI PXI multifunctional acquisition devices were used for controlling and supervising of the engine test bench subsystems, like intake air conditioning system, engine throttle positioning, oil cooling and fuel supply system, evacuation of exhaust gases and additional engine cooling. Generally, the data acquisition was conducted via several data channels (Serial, CAN, AIO, DIO).

Datasets and post-processing

Time and funds-limited projects, such as this one, require slightly different approach to engine test bench run procedure and data acquisition. Control maps were optimized at quasi-stationary operating regimes using "n-const" and "M-const" dynamometer modes [10]. Engine testing was conducted with great respect ofthe procedures defined by the standard ISO 1585 [11]and ISO 15550 [12]with one difference, which is related to the stabilization of the engine operating regime. Because of relatively large number of tester gimes (about 150 regimes for each set of runners) time dedicated for exhaust temperature stabilization was minimized. Instead of waiting for the particular operating regime to become satisfactorily stable, it was decided to perform continuous data logging and after that carrying out more advanced post processing and analysis techniques. In this way, it was possible to preserve engine from excessive wear and obtain sufficiently accurate measuring.

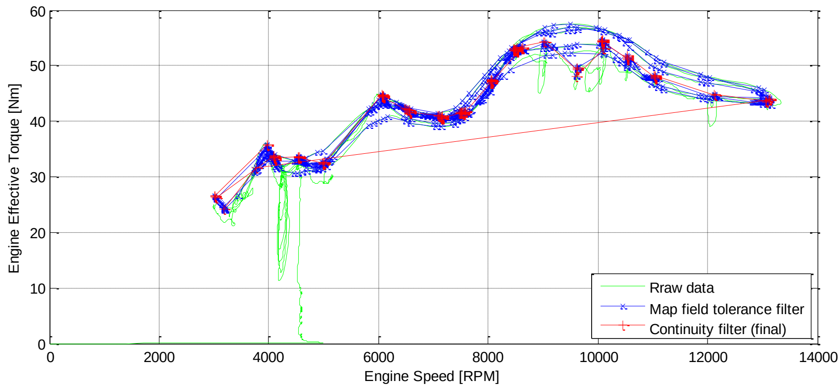

Figure 1 Engine Effective Torque [Nm] over Engine Speed [RPM] at TPS=100%, Runner length 210 mm. Data post-processing and applying filters. Test results of 2013 season

Data sets were acquired by the following test procedure:

– A certain set of intake runners was mounted on the engine;
– All systems of the test bench were checked and the engine was warmed up;
– Dynamometer was set to the required operating mode and a limit for brake torque or RPM was set;
– Engine load was increased slightly to the desired value of throttle opening (throttle and RPM stops are defined by engine control maps). This is done for the whole range of TPS, from 0% to 100%;
– By adjusting dynamometer control parameters, desired engine RPM was reached. Engine speed was varied from 3000 RPM up to 13500 RPM;
– For each pair of TPS and RPM values, ignition advance timing was varied in certain steps to achieve maximum brake torque;
– Injection duration was adjusted in the way of obtaining predefined air to fuel equivalence ratio (AFR).

The same procedure was repeated for all sets of runners. Acquired data sets were recorded independently for each TPS value and for a whole range of RPM. Because of continuous sampling, a large amount of data was obtained and some additional kind of post-processing needed to be applied. Besides moving-average filter, additional ones were generated. Forthcoming analysis was applied only to the data that had been filtered, which refers to the prescribed tolerance of engine speed, throttle position and optimal advance timing. Additionally, one of the conditions was that the filtered data needed to be logged continuously for a certain period of time. In this way, engine testing time was significantly reduced. The engine brake torque data for the engine configuration with 210 mm runner length is used to describe the mentioned methodology and results are shown in Figure 1. All relevant engine data sets were treated in this manner.

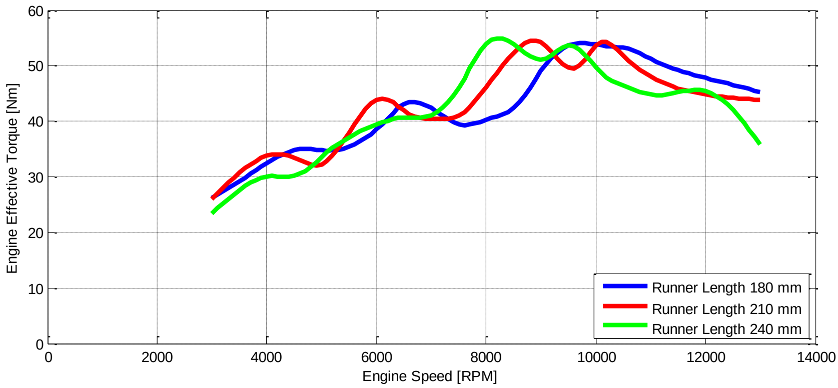

Figure 2 Engine Effective Torque [Nm] over Engine Speed [RPM] at TPS=100% for different Runner Lengths,Final data. Test results of 2013 season

Taking into account the complexity of a racing vehicle, as a whole, and numerous influential factors that affect overall performance, many hours of testing of the entire system have been conducted. With different engine torque curves it is expected the car behavior on the track will be different. Considering different final drive ratios, the tractive effort characteristic was examined in parallel with data analysis obtained during the race. More details about race data log will be shown below. The engine intake manifold in configuration with a 210 mm runner length turned out to be the best option, which was used during the competition.

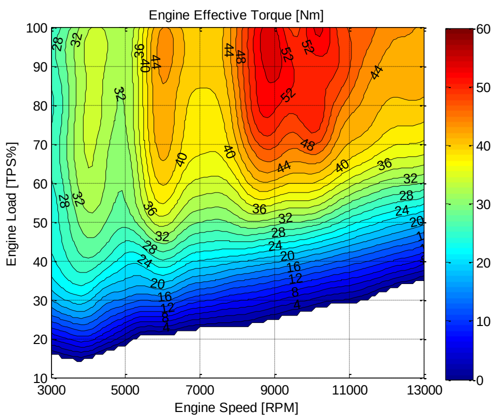

Figure 3 Engine Effective Torque [Nm] as a function of Engine Speed [RPM] and Load [TPS%], Runner Length 210 mm

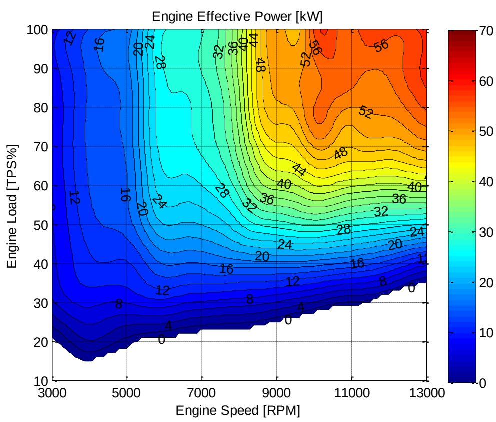

Figure 4 Engine Effective Power [kW] as a function of Engine Speed [RPM] and Load [TPS%], Runner Length 210 mm

Detailed analysis of the obtained data was carried out using self-developed MATLAB codes dedicated to NI LabVIEW *.tdms files processing. The engine universal performance characteristics maps were effectively drawn by implementing the Design and Analysis of Computer Experiments (DACE) [13], a MATLAB approximation toolbox. Some of the experimental results, such as engine torque and power, exhaust gas temperature, air mass flow, manifold absolute pressure, brake specific fuel consumption, ignition timing and injection duration are shown in Figures 3 to 10.

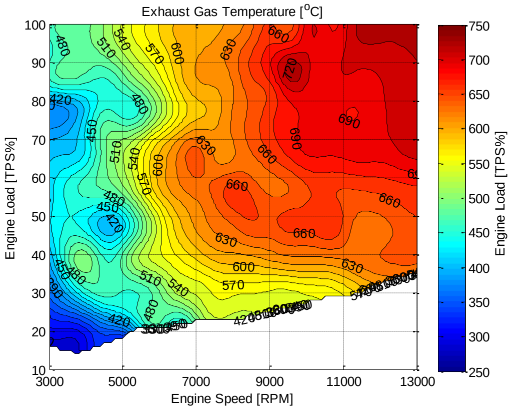

Figure 5 Exhaust Gas Temperature [°C] as a function of Engine Speed [RPM] and Load [TPS%], Runner Length 210 mm

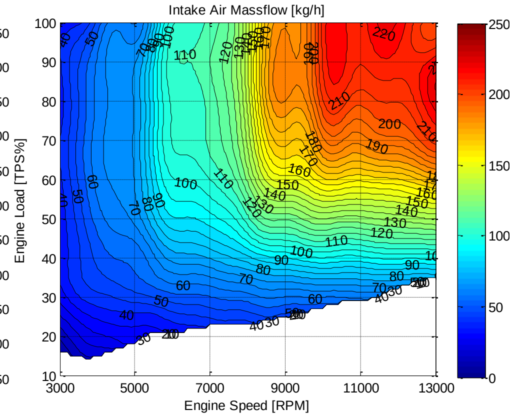

Figure 6 Intake Air Mass Flow [kg/h] as a function of Engine Speed [RPM] and Load [TPS%], Runner Length 210 mm

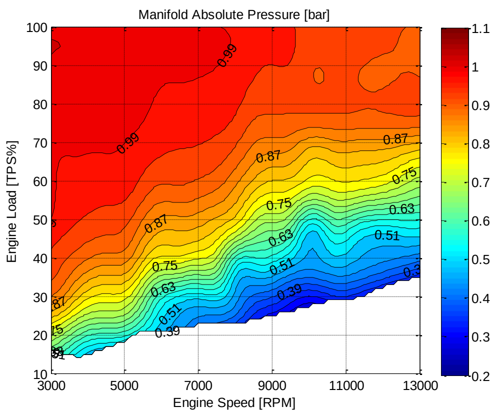

Figure 7 Manifold Absolute Pressure [bar] as a function of Engine Speed [RPM] and Load [TPS%], Runner Length 210 mm

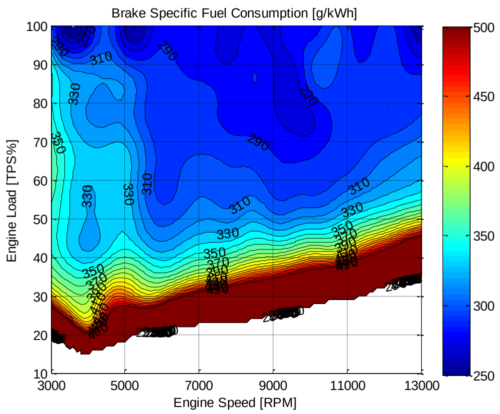

Figure 8 Brake Specific Fuel Consumption [g/kWh] as a function of Engine Speed [RPM] and Load [TPS%], Runner Length 210 mm

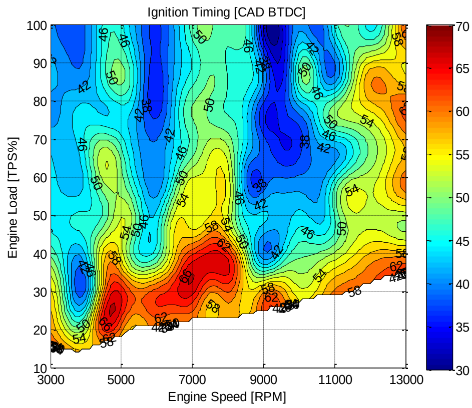

Figure 9 Ignition Timing [CAD BTDC] as a function of Engine Speed [RPM] and Load [TPS%], Runner Length 210 mm

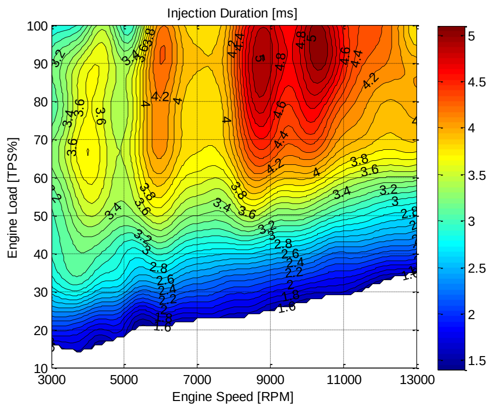

Figure 10 Injection Duration [ms] as a function of Engine Speed [RPM] and Load [TPS%], Runner Length 210 mm

IN-VEHICLE DATA LOGGING AND ANALYSIS

Significant attention was dedicated to in-vehicle data log and analysis of the gathered data. In the first place, the most frequent engine operating regimes needed to be defined because of getting the starting point for the development of the engine mathematical model. Data logging was performed using ECU’s built-in log option combined with E-Race analysis software [14].Simultaneous sampling of 34 different engine and vehicle parameters with a sampling frequency of 10Hz was used. The most important data were the onesrelated to over-time changes of engine speed, throttle opening, lambda reading, water and oil temperatures, driven and undriven wheel speed, etc. Some of the log results acquired at the competition during the race are shown in Figure 11.

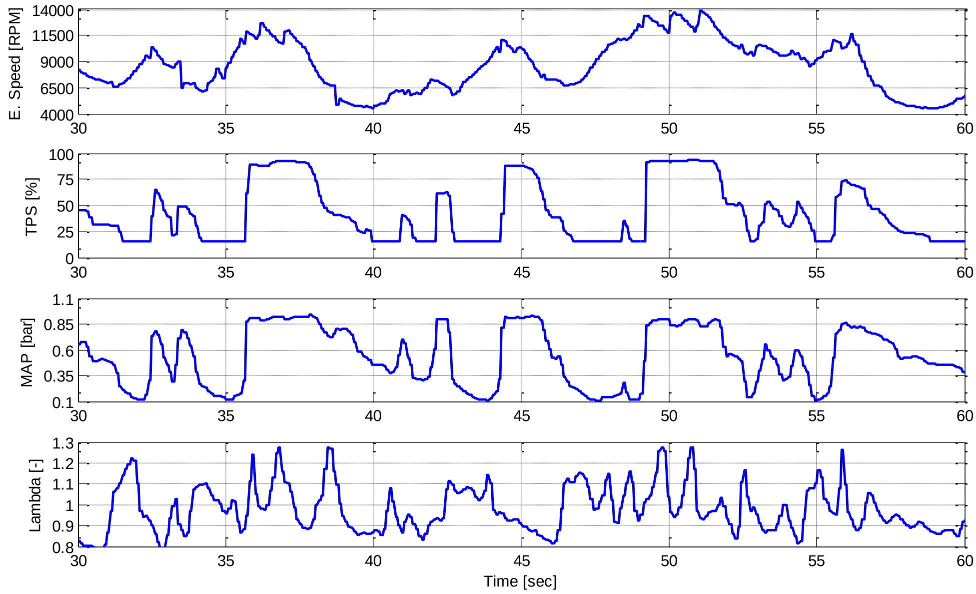

Figure 11 Race track data log. Engine Speed [RPM], Throttle Opening [%], Intake Manifold Pressure [bar] and Lambda reading [-] changing over time during the race

Statistical analysis of the data mentioned provides important guidelines for the forthcoming design and development process. Also, the results of the analysis of the dynamic behavior of the entire system are of great importance. The rate of change of certain parameters, such as engine speed and load, has influenced the CVIM building concept, the way of actuation and further control algorithms. The statistical distribution of engine speed, throttle position and lambda readings during the one complete race, which is 22 km long, is shown in Figure 12.

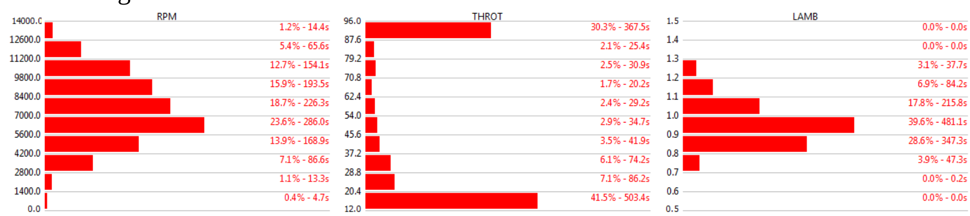

Figure 12 Statistical distribution of relevant engine parameters logged during the race

THEORETICAL APPROACH TO ENGINE RESONANT CHARGING

An approach towards defining optimal intake plenum volume and intake runners length so that the effect of resonant charging could be utilized lies on the basis of Helmholtz resonant theory.

The theory is described in a machine system called Helmholtz resonator, which consists of one spherical cavity with a single tube of defined length and diameter. The main idea of a Helmholtz resonator is that with the right frequency of disturbance on the open end of the tube, the complete system gets into resonance. The equation (1)that defines the frequency needed for getting the system with a known cavity volume, diameter and tube length in resonance is:

$$f_H = \frac{c}{2\pi}\sqrt{\frac{A}{VL}}, \quad (1)$$

where:

- f_H is the resonant frequency[Hz];
- *c*is the speed of sound [m/s];
- *A*is the cross-sectional area of the tube [m^2];
- *V*is the static volume of the cavity[m^3], and
- *L*is the length of the tube [m].

The speed of sound is calculated from the ideal gas equation as:

$$c = \sqrt{\kappa RT}, \quad (2)$$

where:

- *k* is the adiabatic index (equals 1.4 for air [15]);
- *R*is the ideal gas constant (equals 287.1 J/kgK[15]), and
- *T*is the temperature in [K].

From given equations, it can be seen that there is no significant influence of the intake manifold pressure change on the resonant charging via this approach. Resonant frequency f_H, is the frequency of intake valves opening. As known, the frequency of camshaft rotation of a four-stroke engine is equal to half of the crankshaft rotation frequency. Intake air temperature influence was considered taking into account readings from sensors that were installed on the laboratory installation during engine testing. The readings were in the range of 30°C to 50°C. It was agreed that it would be similar to on-track conditions, as races are held in the summer time. Temperature variations affect the calculated speed of sound by no more than 3%, so the complete influence of the temperature change is declared as non-important for the following analysis, noting that future control algorithms should have an integrated temperature compensation. Intake air temperature was only considered for determining injection time compensation, without which the engine would have bad management.

The cross-sectional area of the tube was kept the same as in the previous year (diameter of 40mm), as there was an intention to avoid the possible effect of tube diameter change on the engine effective parameters. The main goal was to evaluate the influence of intake plenum volume and intake runners length variations on the engine effective performance.

The approach to defining needed intake plenum volume (V) and runner length (RL) lied in the development of a MATLAB code for the assumption of resonant fields in a V versus RL map for given engine speed, which was the baseline of the engine work cycle simulation. From data acquired earlier, it was possible to identify the engine working regimes on which the resonant charging phenomenon was utilized. As the tests were performed with three different sets of runner lengths, the resonant charging phenomenon was identified at 9400, 8700 and 8100 RPM, respectively. The next step was to analyze these regimes using the Helmholtz resonant theory equation (1).

The differences that were seen were discussed as the difference between the physical design of the Helmholtz resonator and the intake manifold for a four-cylinder engine.

The firstly mentioned is one-end open system, with spherical volume and one tube, and the other is an open thermodynamic system with one input tube (the intake restrictor section) and four output tubes (leading to the engine cylinders).

Due to the high intake air velocity (the nominal air mass flow was defined as 240 kg/h, which corresponds to 13500 RPM and WOT, after which there strictor chokes), the correlation was defined so that there must be reduction in the in-cavity air volume that is acting as one defined in eq.(1). The trend of this volume reduction is defined for the regimes mentioned, and a resemblance was noted with air-mass flow through the intake manifold. A new variable, ΔVdyn was integrated into an algorithm, so the work could carry on defining resonant fields across the engine work field.

The input volume of the intake plenum was set in the range from 0.1 dm^3 to 6 dm^3, with steps of 0.1 dm^3, from which the needed intake runners length for resonant charging have been identified, as seen in Figure 13:

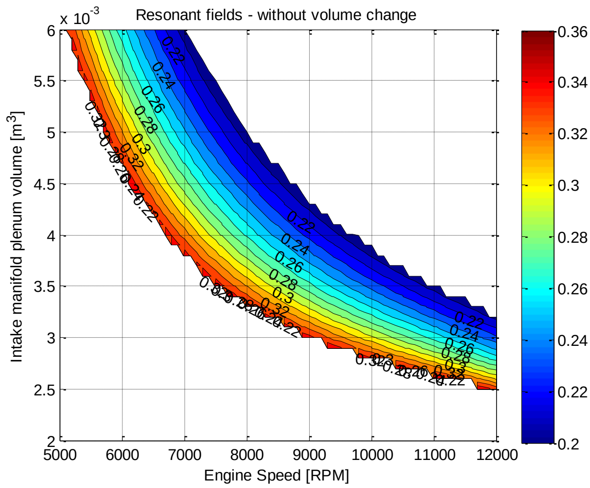

Figure 13 Calculated Runner Length [m] as a function of Engine Speed [RPM] and Intake manifold volume [m^3] without volume change that is present in the physical model of CVIM

The next objective was to define the approach behind the active change of intake runners length, for race track use. The principle is set to be telescopic tubes which would change their length inside the intake plenum volume, as any other principle would produce a need for grave reconstruction of the existing intake manifold concept, with which the benchmark would be lost.

The main problem with the telescopic tubes approach is that when the intake runners extend, the intake plenum volume decreases. As shown in equation (1), the cavity volume and the tube length have the same influence on the resonance frequency.

The effect of the intake manifold geometry change with the change of intake runners length is that the resonant fields, shown in Figure 14, are narrower than those which are calculated with constant volume, as shown in the Figure 13. The physical meaning of the noted problem is that it is needed to elongate intake runners more than it would be needed if the volume was kept constant.

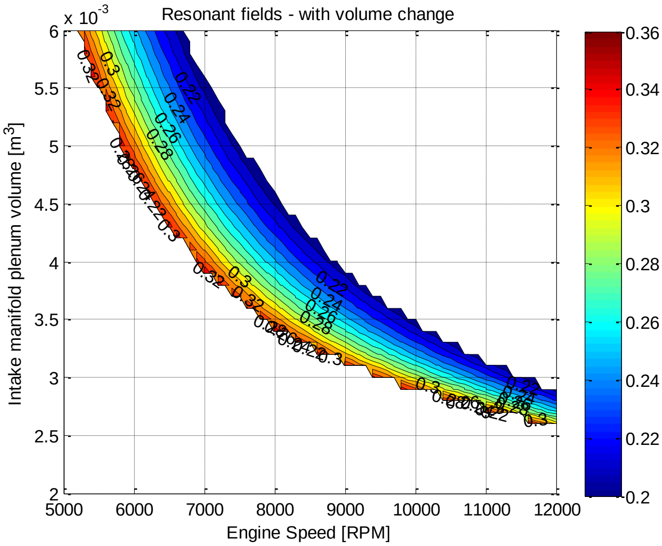

Figure 14 Calculated Runner Length [m] as a function of Engine Speed [RPM] and Intake manifold volume [m^3] with volume change that is present in the physical model of CVIM

The baseline plenum volume for the designed CVIM was set to the level of half of the maximal runners length elongation (stroke), and it was set at 4 dm^3. It was set to this value with the idea of having resonant charging in the widest area shown in the Figure 14, or in the as wide stas possible range of engine speed. Runners length was adopted using earlier discussion to vary from 160 to 260 mm, but during the design process the variable length was reduced to 96mm in total, so the final runners length was in the range of 164mm to 260mm.

ENGINE MATHEMATICAL MODEL

Due to the impossibility of putting the engine on a test bench, it was necessary to perform an advanced engine mathematical model simulation. The mathematical model was set in Ricardo WAVE simulation software. The complete analysis was done for Wide Open Throttle (WOT). Test-bench results were used to calibrate the model of the engine from the previous season. That was a fundamental step for further design and optimization of the CVIM for season 2014. The model calibration was performed for various parameters, especially the engine effective torque, advance timing, air mass flow, A/F ratio, etc.

The first step in the model setting up was mapping of the whole geometry of the intake and exhaust system, such as runner lengths and diameters, volume of the plenum, length and diameters of the restrictor section, the position of the injectors, types of materials used, wall thicknesses, heat transfer coefficients etc. Internal engine geometry such as bore, stroke, connecting rod length, wrist-pin offset and the compression ratio were taken from the manufacturer's specifications [16]. Initial conditions such as exhaust gas, intake air and wall temperatures should be entered as some reasonable values. For the purpose of this project, the values were taken as recommended from the WAVE Knowledge Center [17]. Special attention was given to the plenum geometry, which was meshed from CAD model using the Wave Mesher software.

Because the engine was not indicated during testing, particular attention was given to the Friction Mean Effective Pressure (FMEP) assessment which was calculated with an equation which approximates total friction correlation [18]. The equation is defined by two constants and mean piston speed, i.e. it correlates FMEP and the engine speed linearly. This was proved to be just enough accurate assumption for the purposes of development of the model.

The equation states:

$$FMEP = a + b \cdot Sp \,, \tag{3}$$

Where a and b are friction correlation constants dependent on the type of the engine and S_p is mean piston speed.

The engine heat-release model, i.e. its parameters such as BDUR, CA50, and WEXP were determined using a Single Wiebe model. It was the most appropriate approach to the problem, considering possible options. The equation (4), which represents the Wiebe function [19], is given by:

$$W = 1 - e^{-AWI \cdot \left(\frac{\Delta\Theta}{BDUR}\right)^{WEXP+1}} \,, \tag{4}$$

where:

- W is cumulative mass fraction burned [-];
- $\Delta\Theta$ is crank degrees past start of combustion [CAD];
- $BDUR$ is user-entered 10-90 percent burn duration [CAD];
- $WEXP$ is user-entered Wiebe exponent [-];
- AWI is internally calculated parameter to allow BDUR to cover the 10-90 percent range [-];
- $CA50$ is user-entered 50 percent burn location [CAD ATDC].

Values for BDUR and WEXP were adopted from Blair's findings [20]. The WAVE inputs for Wiebe function operate exclusively – either Start of Combustion (SOC), either CA50[17].The CA50 values were not considered because of existing data for the Start of Combustion (SOC) in WAVE terms or ignition timing in general. In addition, if a user enters both values at the same time, WAVE prefers SOC values. The CA50 was only considered as a control parameter. Blair's recommendation for BDUR parameter was overruled, since they are too low and complete combustion process would have ended even before TDC leading to irrationally high cycle peak-pressure values. So the next step was to find the appropriate BDUR values across the range of RPM at WOT.

Once all relevant data that was available had been set, whether recorded or recommended, the simulation of the model was initialized. Simulations were performed for the regimes from 4000 to 13500 RPM, which was the engine RPM range used in the prior season. The BDUR parameter was varied from 40 to 95 CAD. As previously said, the calibration of the model was conducted, so the appropriate value of BDUR for recorded torque was aimed through the simulation. The results were exported and then the post-processing of those data was carried out in the MATLAB programming environment.

One of the outputs of the engine model calibration were overlapped torque curves at WOT, which are shown in the Figure 15. For the engine speed regimes of interest, a relatively good fit was achieved and this was a starting point for further development of the CVIM.

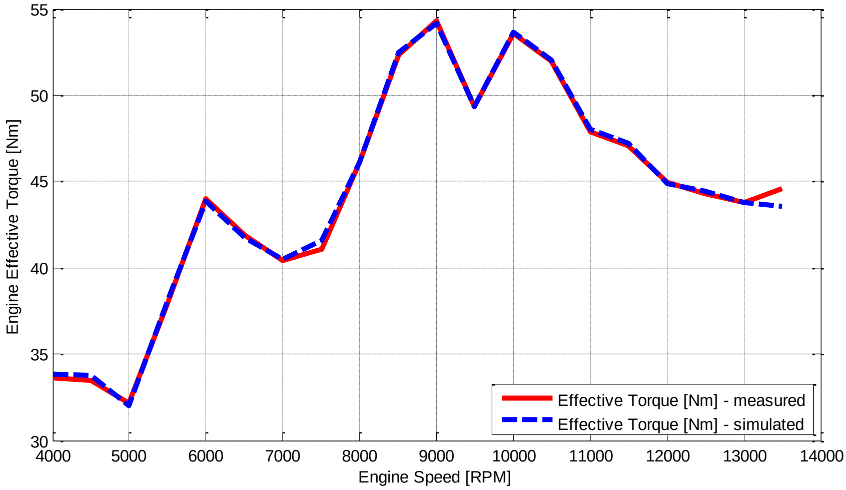

Figure 15 Engine Effective Torque [Nm] over Engine Speed [RPM]. Matching of the simulation results and measured values

After the engine model calibration, the next step was the redesign of the intake and exhaust manifold geometry. The manifolds needed to be optimized in order to improve engine torque characteristics over the wide RPM range and especially between 6000 and 8500 RPM. In this manner, tractive characteristics of the vehicle would be greatly improved.

POST PROCESSING OF DATA OBTAINED FROM WAVE

The outputs from the Ricardo WAVE analysis were effective engine torque characteristics as a function of engine speed, load and runners length. For every pair of engine speed and throttle position, 20 different runners length values were simulated in steps of 5mm, with their repercussion on the plenum volume. One of those sets of effective torque data (given for WOT over the engine speed range from 4000 to 13500 RPM) is shown in the Figure 16.

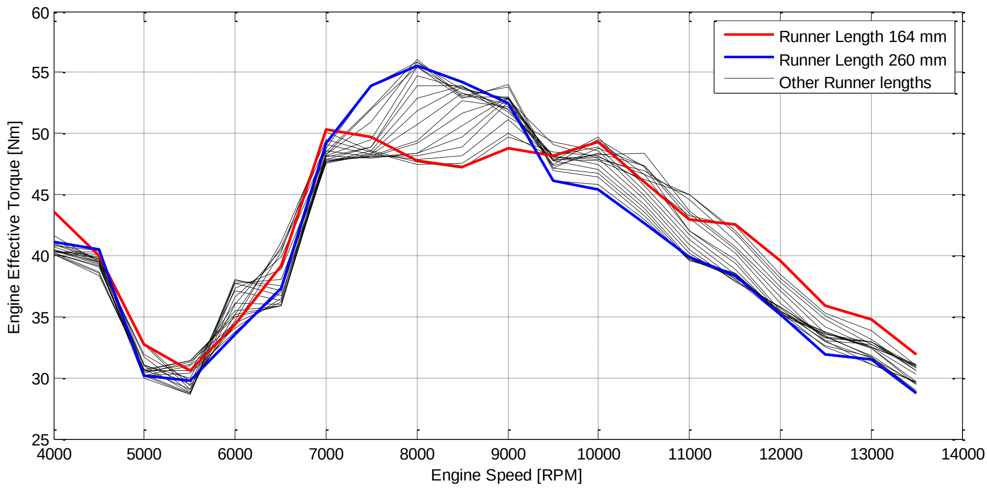

Figure 16 Engine effective torque [Nm] as a function of Engine speed [RPM] and for a range of runner length values simulated at WOT

The approach to determining a control algorithm for runners length variations over engine speed was a multi-step process. The first step was to identify the runners length for the maximum effective torque at the engine speed range previously defined. The next step was to develop a filter so that the change in runners length values over consecutive engine speeds should be observed with an as lower as possible gradient, either positive or negative. The main condition in the filtering process was that the alternative runners length position had an as little as possible influence on the maximum effective torque for the given engine speed.

The first part of the filter consisted of an effective torque map over engine speed and runners length, from which areas with less than 90% of maximum torque at given engine speed were removed . With this approach it was possible to identify the combinations of engine speed and runners length in which the system should not operate. Afterwards, the map was divided into three sections in order to improve the filtration process.

The section of the map in the engine speed range from 9000 to 13500 RPM was identified as one for which the first control algorithm showed that the runners length should be in the upper position, with the tendency of shortening. There were no abrupt changes in control value gradient or its direction, so that part of the filter was set to be the same as the original.

Some minor deviations in the needed runners length position were noticed in the maximal effective torque region, i.e. between 7500 and 9000 RPM. Taking this into account, the analysis showed that there would be no significant difference (<1%),hadthe runners length been kept at a constant level.

Runner lengths for middle and high regimes are mainly linear. However, the most challenging section for the optimization of required variable runners positioning was in the engine speed range from 4000 to 7500 RPM. The same principle of making the control pattern as linear as possible, with minor influence on the engine effective torque, was utilized. Because this part of map was problematic, it was divided into two sections that were simultaneously resolved.

Values for runners length positions are chosen in such a manner so that the effective torque difference is kept under 5% of the potentially maximum value wherever possible and also the consecutive values do not differ more than 20mm. After a detailed analysis, the complete runners length value over engine speed look-up table was defined and finally implemented into the control algorithm of the designed continually variable geometry intake manifold.

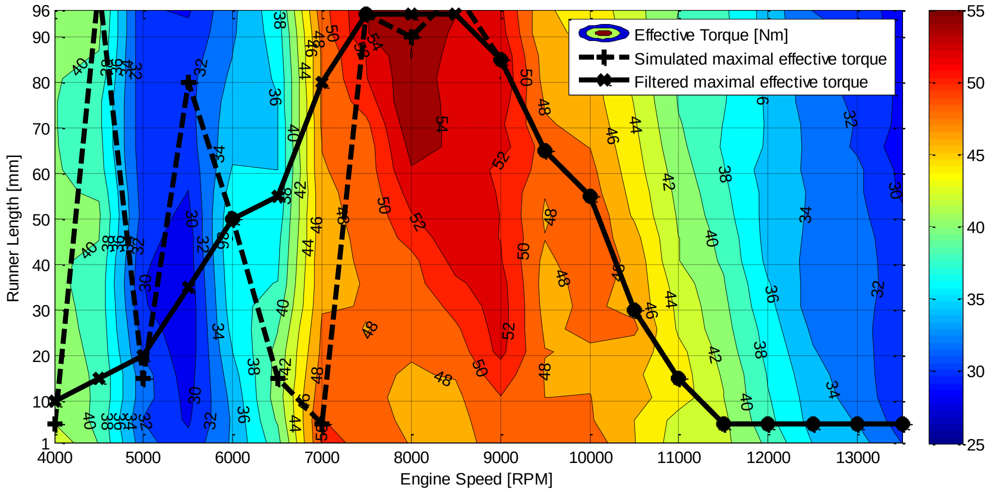

Figure 17 Simulated Engine Effective Torque [Nm] and required Runner Length [mm] values over Engine Speed [RPM] at WOT

Quantitative differences between effective torque and effective power over engine speed from last season's engine testing, as well as the simulated maximal effective torque and power with the implemented CVIM system with raw and optimized RL positioning are shown in the Figure 18:

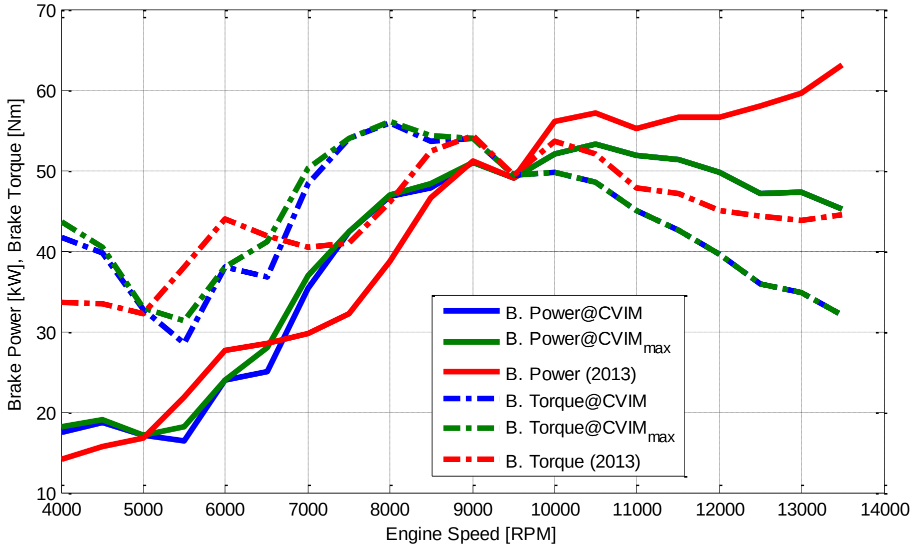

Figure 18 Engine Effective Torque [Nm] and Power [kW] curves over Engine Speed comparison of test and simulation results at WOT

VARIABLE INTAKE MANIFOLD CONCEPT

While designing such a system, considerations regarding the actuation, control, production technologies, reliability and cost are very important. Taking into account the numerous assumptions about weight and speed of movable parts, the forces in the mechanism and the actuation system needed to be defined. For this kind of analysis, the use of LinMot - Designer software [21] was very useful. Generally, actuation by a linear magnetic actuator, DC motor and stepper motor were all considered. The final solution is based on the use of two Futaba S3306MG high-power servo motors and a set of liners and livers. The intake manifold, runners and the restrictor section were made of high resistant ABS plastic using 3D printing technology.

The implemented CVIM control look-up tables are relied on optimized runners length as a function of engine speed and throttle position, but for this study only WOT regimes are considered. After the production and assembly process, a calibration of the physical model needed to be conducted. Control PWM signals were adjusted with an offset because of the need to bring the system in perfect balance.

Before the implementation of the CVIM into the vehicle, a real-time functionality test was carried out. The simulation of control signals was based on the predefined correlation of required runner length over engine speed which was varied over time on the basis of the data logs which were mentioned before.

Rendered CAD models of the intake manifold that was constructed are shown in the Figure 19. On the left-hand side, the intake manifold with an adjustable runner length that was used during engine testing and competition season of 2013 is shown. The middle one and the picture on the right-hand side show the constructed CVIM in the two end positions of the runners with servos position, injector mounts, restrictor section position and throttle body position.

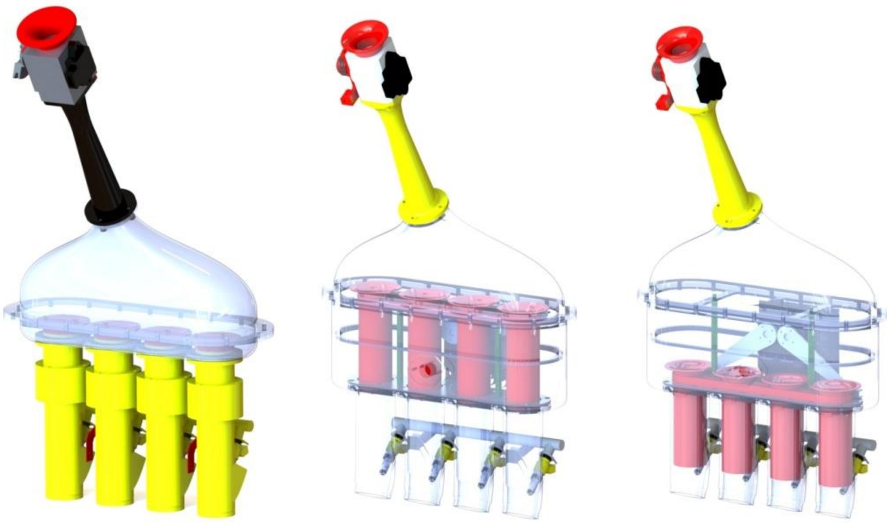

Figure 19 Rendered CAD models of the Intake manifold from the 2013 competition season (left), CVIM with extended runners (middle) - 2014, CVIM with contracted runners (right)-2014

CONCLUSIONS

Engine testing is a very expensive and time consuming process, especially if a large number of operating regimes need to be considered. Different engine speeds and loads, combined with the fuelling, ignition timing and intake runner length adjustments could give a large number of optimal combinations in terms of maximum effective performance.

This is supported by the fact that high-revs engines, such as Yamaha's R6, are very delicate and there is a great probability of an incident occurring if something goes wrong during the testing. On the other hand, data obtained during engine testing are very important for the calibration process of the engine mathematical model.

Several years of development of engine systems intended for racing applications, using this approach, resulted in a high-fidelity engine mathematical model and many useful conclusions.

This paper briefly presents some of the analysis results obtained during the CVIM development process. Generally, simulations of the engine work cycle were performed also for partial load regimes. From the aspect of the engine management system, only the use of optimized look-up tables matters. Regarding this, the correlation between injection timing and effective engine torque was formed based on data obtained during engine testing. Having that in mind, the new injection control map was adjusted for the new power train system.

Plans for the future include performing crank-angle resolved cylinder pressure measurement at a certain number of engine operation regimes. Also, there is a need to perform intake and exhaust ducts indicating in order to achieve better mathematical to physical model matching.

REFERENCES

[1] Group of authors, 2014 Formula SAE® Rules, SAE International, 2014.

[2] Group of authors, Formula SAE Italy & Formula Electric Italy 2014, Italian Automotive Technical Association, 2014.

[3] Group of authors, Formula Student Austria, FSA Rules 2014, 2014 .

[4] Group of authors, Formula Student Germany, Formula Student Combustion Rules 2014, 2014.

[5] Group of authors, Formula Student Hungary, FSH 2014 Rules, 2014.

[6] Group of authors, S Series User Manual, DTA Competition Engine Management Systems, 2012.

[7] S. J. Popović, N. L. Miljić, Četvorokanalni univerzalni modul za kondicioniranje signala MSGA-41, 2007.

[8] P. Mrdja, N. Miljić, M. Kitanović, S. Popović, M. Tomić, Model based approach in Yamaha R6 Formula Student engine control parameters optimisation, Interantional Congress Motor Vehicles & Motors 2012, MVM 2012.

[9] P. Mrdja, V. Petrović, N. Miljić, S. Popović, M. Kitanović, Combustion parameters calibration and intake manifold redesign for formula student Yamaha YF-R6 engine, International Conference on Accomplishments in Electrical and mechanical Engineering and Information Technology, DEMI 2013.

[10] Group of authors, Bedienungsanleitung Carl Schenck W130, 1984.

[11] Group of authors, ISO 1585:1992, Road vehicles - Engine test code - Net power, 2010.

[12] Group of authors, ISO 15550:2002 Internal combustion engines - Determination and method for the measurement of engine power - General requirements, 2010.

[13] S. N. Lophaven, H. B. Nielsen, J. Sondergaard, DACE - A Matlab Kriging Toolbox, 2002.

[14] Group of authors, E-Race v3 User Manual, XAP Electronics, 2008.

[15] B. Vasiljević, M. Banjac, Mapa za termodinamiku - Mašinski fakultet Beograd, 2008.

[16] Group of authors, Yamaha YZFR6V(C) Service manual, 2008.

[17] Group of authors, WAVE Knowledge Center v2013.1 Ricardo Software. 2013.

[18] M. Tomic, Fundamentals of the Internal Combustion Engines, Handouts as addition to the lectures, 2011.

[19] D. Cordon, C. Dean, J. Steciak and S. Beyerlein, One-dimensional engine modeling and validation using Ricardo WAVE, Final Report, University of Idaho, 2007.

[20] Blair, Gordon P., Design and Simulation of Four-Stroke Engines. Society of Automotive Engineers, 1999.

[21] Group of authors, LinMot Designer tutorial, NTI AG, 2013.

ENGINE CRANKSHAFT SPEED MEASUREMENT ERROR COMPENSATION

Nenad Miljić[1], Slobodan J. Popović , Marko Kitanović

UDC:621.431.73:53.088.6

ABSTRACT: Engine speed signal contains valuable and rich content information about the engine working process. Measurement of the engine speed is usually carried out by sensor wheels mounted on the crankshaft. Measurement errors are mostly influenced by geometric tolerances of the engine speed sensor wheel as well as by its radial run-out. In order to avoid the occurrence of this systemic deviation, in the lab and highest accuracy engine speed measurements are usually conducted by means of incremental encoders, radially and axially fixed to the crankshaft with the anti-twist safeguard toward the crankcase. This paper shows how this type of engine speed measurement, which is considered to be the most accurate, is prone to systematic errors as well. The influence of the kinematic parameters of the encoder - crankcase linkage, on the error occurrence is discussed as well as suggested methods for systematic deviation parameters identification and engine crankshaft angular speed error compensation.

KEY WORDS: engine speed measurement, measurement error, crank angle optical encoder, IC engine

KOMPEZACIJA GREŠKE MERENJA BROJA OBRTAJA KOLENASTOG VRATILA MOTORA

REZIME: Signal broja obrtaja motora sadrži značajne i brojne podatke o procesu rada motora. Merenje broja obrtaja motora se obično izvodi senzorima postavljenim na kolenasto vratilo. Greške merenja su uglavnom pod uticajem geometrijskih tolerancija senzora broja obrtaja motora kao i njihove centričnosti. Da bi se izbegla pojava ovog sistemskog odstupanja, u laboratoriji se merenja visoke tačnosti broja obrtaja motora obično izvode primenom inkrementalnih enkodera, radijalno i aksijalno fiksiranih na kolenastom vratilu kako bi se izbeglo uvijanje u odnosu na kolenasto vratilo. Ovaj rad pokazuje kako ovaj tip merenja broja obrtaja motora, koji se smatra najtačnijim, dobro eliminiše sistemske greške. Uticaj kinematiskih parametara enkodera na pojavu greške je tema rasprave kao i predložene metode za identifikovanje sistematskih odstupanja parametara i kompezacija greške ugaone brzine radilice.

KLJUČNE REČI: merenje broja obrtaja motora, greška merenja, ugao kolenastog vratila, optički enkoderi, IC motor

[1] *Received August 2014, Accepted September 2014, Available on line, June 2015*

Intentionally blank

ENGINE CRANKSHAFT SPEED MEASUREMENT ERROR COMPENSATION

Nenad Miljić[1], *Slobodan J. Popović*[2], *Marko Kitanović*[3]

UDC:621.431.73:53.088.6

INTRODUCTION

Engine crankshaft speed is a parameter which is often unavoidable to be used in numerous internal combustion engine applications. Depending on the application, this parameter can be used as an averaged or discrete instantaneous value. In applications which involve a monitoring of engine speed, this parameter is usually time averaged, but in more demanding applications the measurements of engine speed are often averaged on per cycle or per revolution period. When used as an input parameter for the control of internal combustion engines, as a crucial and indispensable parameter, it is measured in angle based resolution, thus becoming a signal which gathers information on instantaneous engine crankshaft speed.

Demands for a high quality and accuracy of the measured engine speed become stricter in more sophisticated research applications both in terms of signal amplitude and resolution. This is particularly true in research which is related to the identification of the dynamic parameters of crankshaft or, more general, complete crankshaft mechanism. It is well known fact that the combined action of gas and inertial forces, within an internal combustion engine, generate highly varying torque, which, coupled with the torsionally elastic behaviour of the engine crankshaft, produce rapidly changing instantaneous engine speed. This complex picture of instantaneous engine speed contains valuable information about engine processes and it is therefore widely used in a vast variety of engine applications - from engine control to engine diagnostics.

During the past decades a lot of effort is put in research of methods which can provide the needed accuracy in the measurement of engine crankshaft angular speed. The problem in defining the most appropriate method which leads toward the highest possible measurement accuracy is in the necessity to solve multiple and rather diverse issues. Moreover, as usual in the engineering practice, researchers are additionally and always faced with the common demands about keeping the costs of measurement chains as low as possible. Although mentioned problems are common for all types of engine speed measurement devices, it is a general belief that the usage of more sophisticated and expensive devices, like optical encoders, can solve almost all of these problems. This research shows that above mentioned assumption can be misleading and that serious

[1]*Nenad Miljić, Assistant Professor, Internal Combustion Engines Department, Faculty of Mechanical Engineering, University of Belgrade, KraljiceMarije 16, 11120 Belgrade 35, Serbia, nmiljic@mas.bg.ac.rs*
[2]*Slobodan J. Popović, Assistant Professor, Internal Combustion Engines Department, Faculty of Mechanical Engineering, University of Belgrade, KraljiceMarije 16, 11120 Belgrade 35, Serbia, spopovic@mas.bg.ac.rs*
[3]*Marko Kitanović, Research and Teaching Assistant, Internal Combustion Engines Department, Faculty of Mechanical Engineering, University of Belgrade, KraljiceMarije 16, 11120 Belgrade 35, Serbia, mkitanovic@mas.bg.ac.rs*

measurement errors can be made even by using optical encoders – despite their high geometrical tolerances and design quality.

SOURCES OF ANGULAR SPEED MEASUREMENT ERRORS

Angular speed measurement basics

The key component of an angular speed measurement chain is a teethed or slotted wheel mounted on a crankshaft. Teethes or slots are used as a markers for generating of digital signals which are further used for triggering and stopping of the time period measurements between successive signals. Number of teethes Z defines the angular increment φ_0 of the crankshaft which can be detected and is firmly related to the capabilities of measuring instantaneous angular speed.

$$\varphi_0 = \frac{2\pi}{Z}, \tag{1}$$

Measurement of the time period T_m needed for the angular movement of the crankshaft between two succeeding angular increments gives averaged angular speed on that (i-th) interval:

$$\omega_m(i) = \frac{2\pi}{T_m(i) \cdot Z} i = 0 \dots Z-1, \tag{2}$$

The measurement of the time period T_m is usually done by counting the number of impulses N of the digital pulse train with reference frequency f_0. The goal of this procedure is to quantise time period T_m into product $N \cdot T_0$ (where $T_0 = 1/f_0$). This quantisation gives the discrete, and thus approximate, averaged angular speed on a measured interval - ω_q. The relative error of this approximation can be evaluated as:

$$\epsilon_\omega = \frac{\left|\frac{\varphi_0}{N \cdot T_0} - \frac{\varphi_0}{T_m}\right|}{T_m} = \left|\frac{T_m}{N \cdot T_0} - 1\right|, \tag{3}$$

The absolute value of the quantisation error has to be smaller than quantisation time interval:

$$|T_m - N \cdot T_0| \leq T_0, \tag{4}$$

Therefore an estimation of the relative quantisation error can be expressed as:

$$\epsilon_\omega \leq \frac{1}{N} = \frac{1}{N \cdot T_0 \cdot f_0} = \frac{\omega_0}{\varphi_0 \cdot f_0}, \tag{5}$$

The quantization error depends on the angular speed itself and, at higher engine speeds, it can be improved by increasing the reference signal frequency f_0 or by enlarging the angular interval between increments φ_0. The latter measure has its drawbacks since the enlargement of the measuring interval decline measurement resolution. Smaller number of teethes i.e. larger angular increments gives not only low resolution in instantaneous speed measurements, but also in crankshaft angular position tracking which is important in engine control applications. These problems can be solved by using additional layer in sensor signal processing chain by producing multiple micro-ticks during one angular interval [2].

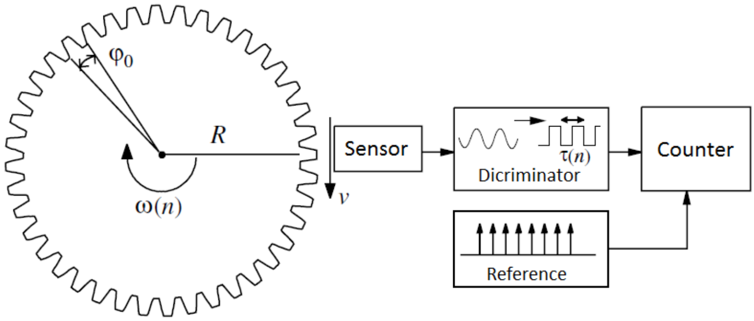

Figure 1 Measurement chain for period based measurement of angular speed [1]

Mechanically introduced measurement errors

Measurement errors, which can be exceptionally larger than those introduced by quantisation process have an origin in geometrical irregularities of measurement wheels or in the undesirable kinematics of the sensor elements. When the speed measurement is based on the usage of teethed wheel, error which is often introduced is a consequence of the radial run-out of the wheel.

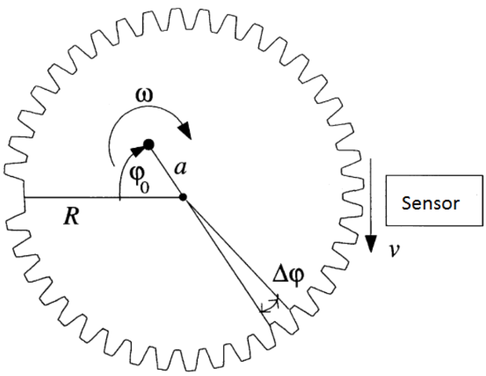

Figure 2 Angular speed measurement errors due to measurement wheel run-out[1]

The sensor, which is static, detects relative speed as:

$$v(i) = \omega \cdot (R - a \cdot \sin(i \cdot \Delta\varphi - \varphi_0)), \tag{6}$$

i.e. the measured angular speed:

$$\omega_m(i) = \frac{v(i)}{R} = \omega \cdot \left(1 - \frac{a}{R} \cdot \sin(i \cdot \Delta\varphi - \varphi_0)\right), \tag{7}$$

where parameter a is the wheel eccentricity (run-out value) and R is a wheel base radius.

When known, parameters a and R can be directly used for the calculation of the measured angular speed correction. In practice, this parameter should be identifiedand this can be achieved by measuring the angular speed of the wheel by providing constant shaft speed. This is, in most cases, rather unpractical approach on the engine and therefore other methods are developed and used. Excellent results can be achieved by driving the engine on regimes where the influence of the gas torque on the engine speed can be minimised as much as possible e.g. during short period of engine fuel cut-off and crankshaft deceleration affected by external engine load[3]. When measurements are made the unknown kinematic parameters can be identified by means of least squares method [1].

Besides measurement wheel run-out problem, additional errors can be introduced through unequally spaced increments on a wheel. These errors are almost unavoidable due to mechanical tolerances of teethed wheels in the production process. This mechanically introduced errors can be compensated through additional signal processing and previous deviation parameter identification. There are different approaches and parameter identification methods. Simple and straightforward compensation parameters estimation is suggested by Kiencke in [1], while Fehrenbachet. al. proposed method which is based on the energy balance equation of the crankshaft mechanism and is well described in [4], [5] and [6]. A similar approach is also used by Rämisch in [7].

When using toothed wheel, mounted on the crankshaft, with statically mounted Hall or variable reluctance sensor, for the angular speed measurement, a compensation of the error due to above mentioned mechanical problems is almost unavoidable. Integral and precise design of a typical industrial type optical incremental encoder and its usage should eliminate this problem with its nature. Nevertheless, errors in measuring crankshaft speed can be still encountered due to several reasons.

Optical incremental encoders are typically mounted on the engine crankshaft in two manners – as directly or indirectly attached. In one of them the encoder is statically mounted in front of the crankshaft and indirectly connected to by means of a torsionally stiff coupling. Problems encountered in this configuration are usually related to the fact that the coupling, which stiffness is not infinite, dynamically modifies and distorts the crankshaft motion [8].

Optical encoder, used in this research, was radially and axially fixed to the crankshaft (direct connection), while the encoder's stator motion was disabled by means of the anti-twist safeguard toward the crankcase. This configuration is often believed to be the superior one in terms of measurement precision and accuracy and is widely used in research applications on engine test benches. Although, this configuration is very sensitive to a mounting faults and this paper's motivation is mostly to emphasize how much this type of faults can introduce huge errors while measuring instantaneous engine crankshaft speed. The proposed method for a correction of the measured engine speed and encoder mounting errors compensation is developed and applied during a research on a 1.4 litres 4-cylinder engine (produced by DMB and very similar to FIAT 1372 ccm SOHC Engine).

CRANK ANGLE ENCODER – MOUNTING ERRORS COMPENSATION

Figure (3) shows an example of the measured angular speed on one of particularly interesting working points. The chosen working point is in the area of middle range engine speed at relatively high load – area in which gas torque dominates and prevails over inertial torque components. Within that engine working area, it is common to expect a picture with four similar engine speed peeks within a complete engine cycle. As evident, the recorded picture looks quite different and this can originate either from the engine itself, if the cylinders differ in energy contribution, or from faulty engine speed measurement. Each of four main oscillation shapes corresponds to a single cylinder activity and there should be noticed slight differences between them as a natural consequence of interference of crankshaft's dynamical behavior. It can be noted that engine speed fluctuation on cylinders no. 1 and 4 (firing order 1-3-4-2) are much higher than those on cylinder 2 and 3. Since no other parameters measured on the engine did not indicate any problems in difference in cylinder energy contribution the suspicion led to measuring deviation which is periodic over a single crankshaft revolution. Moreover, the spotted problem looked very similar to an error produced by a run-out of the measuring toothed wheel.

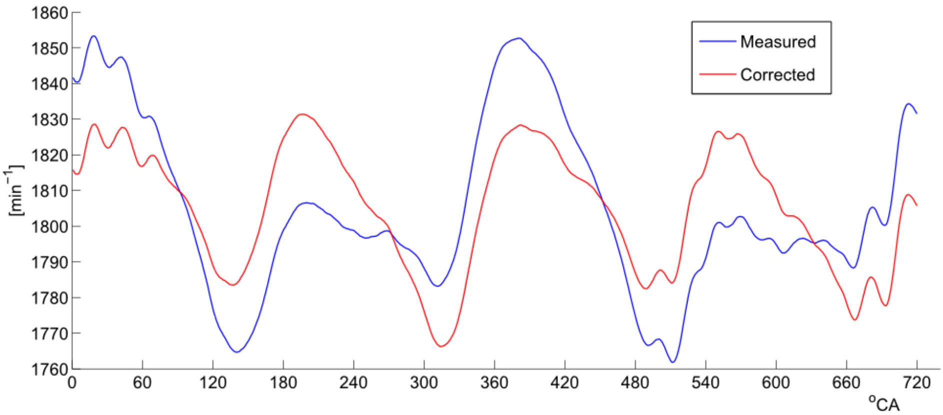

Figure 3 Measured and corrected angular speed – an example (DMB 1.4, n=1800 min^{-1}, p_e=6 bar)

Figure (4) shows the crank angle encoder, used for measurement, mounted on the free end of the crankshaft. The connection between the encoder and the crankshaft is realised in the usual manneron almost exactly the same way as on the Kistler type engine crank angle encoders. The encoder's stator motion is disabled by fixing a secure arm to the adjustable linkage, which is placed between the arm and engine crankcase. The fixing linkage consists of two spherical joints and adjustable length screw rod, thus enabling the wide possibilities in fixing the encoder's secure arm to the most suitable point on the crankcase.

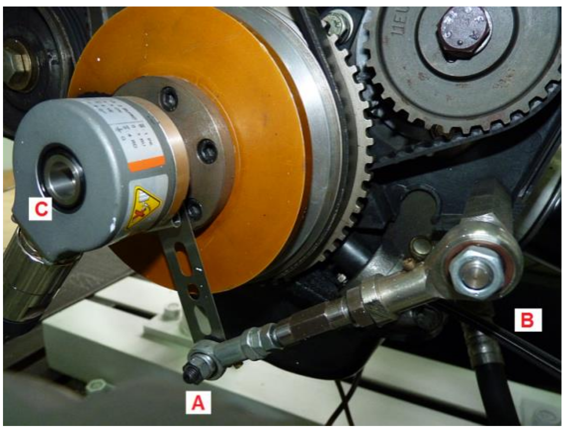

Figure 4 Crank angle encoder mounted on the crankshaft's free end

Due to the tight tolerances used in encoder assembly, the typical run-out of the optical disk is a problem which cannot be expected from this type of device. But, as will be shown, slight radial misalignment between the encoder and crankshaft axis can lead to a circular motion of the complete encoder assembly. This motion, constrained by secure arm and fixing linkage kinematic chain causes a relative motion between the optical disk and encoder's stator which consequences as false crankshaft position reading what further influences angular speed measurement.

Direct mounted single body encoder kinematics

The kinematics of the crank angle encoder which is exposed to the radial run-out motion is explained on figure (5) on which "C" marks the crankshaft axis, "B" marks the attachment point (spherical joint) of the encoder linkage to the crankcase and "A" marks the position of the other spherical joint between the encoder's arm and linkage rod. In order to make analysis easier, the schematic is built around coordinate system xCy. Some arbitrary initial position of the encoder can be chosen but, it is convenient to choose the position in which axis center "C", encoder center "E1", and linkage endpoint "A" are collinear. The chosen initial position of the encoder body is highlighted with circle "k_o" which is intentionally positioned eccentrically from crankshaft axis i.e. the center of circle "k_o" is positioned in the eccentricity circle "k_e". The fixed distance between crankshaft axis and anchoring point on the crankcase "BC" is marked with letter "d".

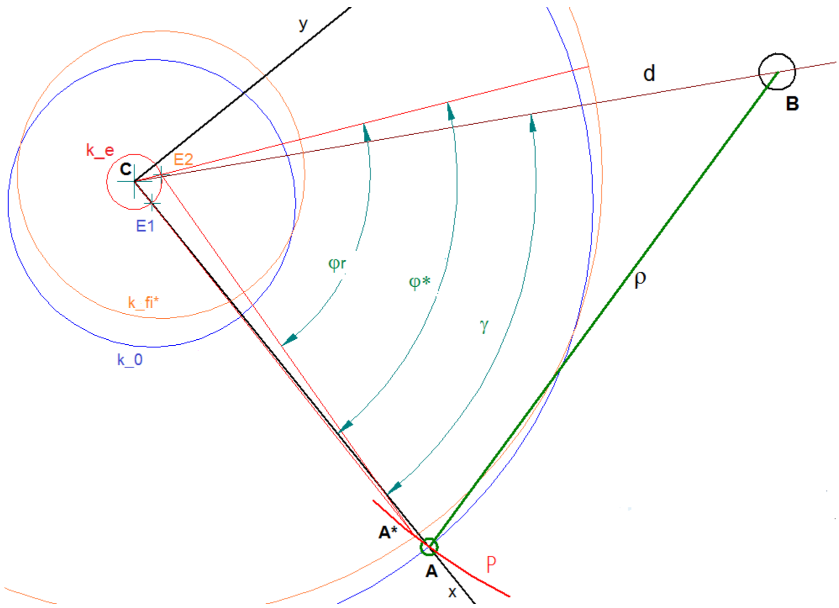

Figure 5 Kinematics of angle crank encoder exposed to run-out motion

When the eccentricity is present, the movement of the encoder's stator can be explained as a complex virtual combination of two simpler motions:

The primary one, during which encoder body follows and rotates together with its rotor (optical disk) and crankshaft. During that angular movement, described with angle φ^* whole encoder rotates to a new position where its center takes position at point E2. Both E1 and E2 points belong to circle "k_e" i.e. they are equidistant from the crankshaft centre point „C" by eccentricity radius e ($CE_1 = CE_2 = e$).

Secondary motion through which the encoder's stator revolves back, with fixed rotor, around point "E2" for angle φ_r in order to "connect" point A of the secure arm with the end of the linkage rod BA. It is assumed that the linkage rod length ρ and secure arm length R are constant and notdeformable. The consequence of the radial run-out of the complete encoder body is the reposition of the spherical joint from point “A” to point “A*” which forces a rotation of the linkage rod BA around point B.

From one side, connecting point “A” is able to rotate along arc “p” with radius ρ (circumscribed from the point “B”). On the other side, belonging to encoder’s secure arm, the point “A” has to be a part of the circle circumscribed from the centre of encoder – point “E” with radius R. Thus the position of the encoder stator is defined by the intersection of this circle and the arc p. The direct effect of the run-out of encoder body is the inequality of above described angles φ^* and φ_r with a difference which oscillates between minimum and maximum value over each crankshaft revolution. The angle difference is converted into the relative motion between the encoder’s stator (which contains the optical sensors) and its rotor (optical disk) and this angle difference time derivative is an angular speed component which interferes with the measured speed and appears as an error (figure 3).

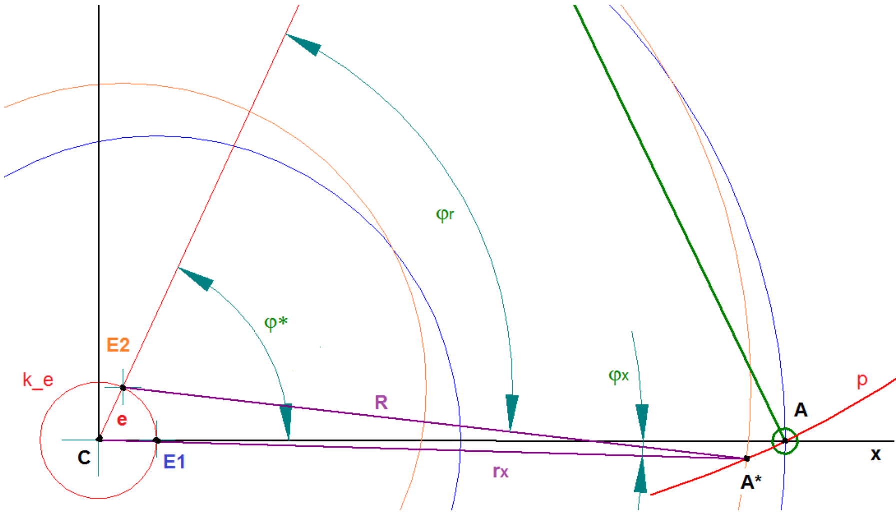

Figure 6 Relation between the angular movements of encoder’s stator and rotor

If the point C is an origin of the polar coordinate system in which the polar distance can be designated as r and position angle as φ (measured from half-line Cx) than the arc p can be described with the following equation (fig. 6):

$$-r^2 + 2 \cdot r \cdot d \cdot \cos(\varphi - \gamma) = -\rho^2 + d^2, \tag{8}$$

The equation of the encoder body circle, rotated for the angle φ^* in the “new” E2 position states:

$$r^2 - 2 \cdot r \cdot e \cdot \cos(\varphi - \varphi^*) = R^2 - e^2, \tag{9}$$

With an assumption that the run-out value e is already known, it is possible, by eliminating the variable r from the system of equations **Error! Reference source not found.** and **Error! Reference source not found.**, to solve the system by variable φ and to identify the exact angular position φ_x of point A*.

Angular difference, defined as $\Delta\varphi_{err} = \varphi_r - \varphi^*$, corresponds to the relative angular movement of encoder’s stator due to encoder run-out. Evaluation of its first order time derivative gives a value which should be used for measured angular speed correction through simple addition. Geometrical relations, which can be spotted on figure 6 give the following equation:

$$\Delta\varphi_{err} = \varphi_x + \arcsin\left(\frac{e}{R}\cdot\sin(\varphi^* + \varphi_x)\right), \tag{10}$$

By using eq. **Error! Reference source not found.** it is possible to evaluate the “error” in measured crankshaft angular position for each value of crankshaft position φ^* on complete revolution period, i.e. for $\varphi^* \in [0 \cdots 2\pi]$.

The run-out value e as well as the angular position φ_{ref} of the polar coordinate system used during equation derivation cannot be determined in advance – it should be identified. For an illustration the angle φ_{ref} used in figure (5) have a value of zero, but in practice it can take a numerous values from an angular interval which is specific for each particular encoder mounting disposition.

In order to identify the unknown parameters e andφ_{ref}, it is necessary to provide representative or reference angular speed measurement data. This can be obtained through measurements on particular engine regimes (like those with shortly introduced misfire or steady-state cranking). Data from other regimes can be used also but only by relying on the assumption that the energy contributions from all engine’s cylinders are equal. The latter approach can be very practical and useful, especially when used on engine’s working points with low COV (coefficient of variation) values.

CASMA filter as tool for run-out parameter identification

The evaluation of the energy contribution of each engine cylinder is a common practice often used in engine diagnostics. It is used for detecting of unequally injected fuel quantities among different cylinders, or to detect a misfire on a particular cylinder. One of very efficient methods for evaluating the cylinder contribution is developed by Schmidt [9]and called CASMA (Crank Angle Synchronous Moving Average) filter.

CASMA calculations are based on the assumptions that the crankshaft is rigid and that entire crankshaft mechanism can be simplified as a single rotating mass with the equivalent moment of inertia J_{ekv}. Upon these assumptions the crankshaft motion equation can be presented in simplified form:

$$\mathrm{J_{ekv}}\cdot\frac{d\omega}{dt} = \sum M_i, \tag{11}$$

Where M_i are torque components which originate in gas and friction forces, external and auxiliary loads as well as in inertial torques. Every of this torque components can be evaluated as the sum of two superposed signals – one of which is periodical and other with a constant value:

$$\mathrm{M_i}(t) = \bar{M}_i(t) + \tilde{M}_i(t), \tag{12}$$

The characteristic torque period in a 4-cylinder engine is 180° i.e.:

$$\tilde{M}_i(\varphi(t)) = \tilde{M}_i(\varphi(t) + \pi), \tag{13}$$

The mean value of the torque, on the π length interval can be calculated as:

$$\frac{1}{\pi}\cdot\int_{\alpha}^{\alpha+\pi}\left(\sum M_i\right)\cdot d\varphi = \frac{J_{ekv}}{\pi}\cdot\int_{\alpha}^{\alpha+\pi}\dot{\omega}\cdot d\varphi = \frac{J_{ekv}}{\pi}\cdot\int_{\alpha}^{\alpha+\pi}\omega\cdot d\omega, \tag{14}$$

A Work of oscillatory torque components, over an interval of periodicity is equal to zero i.e.:

$$\int_{\alpha}^{\alpha+\pi} \widetilde{M}_i \cdot d\varphi = 0, \tag{15}$$

That, actually, simplifies the left side of the equation **Error! Reference source not found.** to the difference between works of mean value gas torques W_g and “constant” value torques originating from the friction forces and external loads W_{const}:

$$W_g\Big|_{\alpha}^{\alpha+\pi} - W_{const} = \Delta \mathrm{E_{kin}}|_{\alpha}^{\alpha+\pi} = \frac{J_{ekv}}{2} \cdot (\omega^2(\alpha+\pi) - \omega^2(\alpha)), \tag{16}$$

The difference, defined by the equation **Error! Reference source not found.**, will be equal to zero if the working process on that interval is quasi-stationary i.e. if its mean value is constant. If the energy contribution of one or more cylinders differs that will distort the mean value of the torque and it will be not constant any more on the periodic interval. Thus, the value of the expression **Error! Reference source not found.** can be used as an indicator of the work balance between cylinders. The greater is the value of this indicator the greater is the difference of works between cylinders.

According to the equation **Error! Reference source not found.**, and the fact that the time derivate of the angular speed can be treated in the same way as the torque in equation **Error! Reference source not found.**, the difference **Error! Reference source not found.** can be expressed as:

$$\Delta \mathrm{E_{kin}}|_{\alpha}^{\alpha+\pi} \sim \frac{1}{\pi} \cdot \int_{\alpha}^{\alpha+\pi} \bar{\dot{\omega}} \cdot d\varphi, \tag{17}$$

In other words, the balance indicator is proportional to the area beneath the angular speed on the interval of periodicity, filtered with the moving average. This conclusion implies that the indicator can be calculated even in dynamical regimes during which the cycle averaged speed is not constant.

If the sampling interval has a length ofΦ_s, the number of sampled points on the angular interval$\Phi_w = 180^o\, CA$, equals $M = \Phi_w / \Phi_s$. Therefore, the equation **Error! Reference source not found.** when discretised into the sampling resolution domain can be evaluated as:

$$\begin{aligned} \Delta \mathrm{E_{kin}}|_{\alpha}^{\alpha+\pi} &\sim \frac{1}{\pi} \cdot \sum_{\nu=0}^{M-1} \dot{\omega}\big((k-\nu)\cdot\Phi_s\big) \cdot \frac{\pi}{\Phi_s} \cdot \Phi_w \\ &= \frac{1}{M} \cdot \sum_{\nu=0}^{M-1} \dot{\omega}\big((k-\nu)\cdot\Phi_s\big), \end{aligned} \tag{18}$$

CASMA algorithm calculates the angular acceleration $\dot{\omega}$ as:

$$\bar{\dot{\omega}}(k) = \omega(k-1) + \frac{\omega(k) - \omega(k-M)}{M}, \tag{19}$$

When the argument is the measured angular speed, according to eq. **Error! Reference source not found.**, the acceleration can be evaluated as:

$$\dot{\omega}_{meas}(k) = \frac{\sum_{\nu=0}^{M-1} \omega_{meas}(k-\nu) - \sum_{\nu=0}^{M-1} \omega_{meas}(k-\nu-M)}{\pi} \cdot \sum_{\nu=0}^{M-1} \omega_{meas}(k-\nu), \tag{20}$$

Since the angular speed is determined by period measurement (counting the number of reference clock impulses arrived during the period interval), the time duration of the period over 180° CA can be evaluated as:

$$\hat{\hat{T}}(k) = \frac{\sum_{\nu=0}^{M-1} n_{imp_{ref}}(k-\nu)}{f_{ref}}, \tag{21}$$

Where f_{ref} is the reference clock frequency and $n_{imp_{ref}}(k)$ is the number of reference impulses arrived during k-th moving period of 180° CA.

Thus the mean value of the angular speed over k-th period can be expressed as:

$$\hat{\hat{\omega}}(k) = \frac{\pi}{\hat{\hat{T}}(k)}, \tag{22}$$

The overall result of a CASMA filter is a residue$r(k)$ which indicates the existence of energetic contribution differences between cylinders:

$$r(k) = \frac{\hat{\hat{\omega}}_{meas}(k) - \hat{\hat{\omega}}_{meas}(k-M)}{\pi} \cdot \hat{\hat{\omega}}_{meas}(k), \tag{23}$$

Now, having the all needed tools, the crank angle encoder run-out can be determined using the following procedure:

1. For initially assumed values of $[e_0 \quad \varphi_{ref_0}]$ the calculation of the corrective angle $\Delta\varphi_{err}$ is done and this value is used for the initial correction of the measured angular speed.
2. The corrected angular speed has to pass further as an argument to the CASMA algorithm in order to calculate the residue vector r
3. The residue value contains the most important information about differences between cylinders energy contribution. Since it is assumed that there is a minimum difference between cylinders energy contribution the value of this residue indicates indirectly how good was the guess of values$[e \quad \varphi_{ref}]$.
4. In order to estimate the correct run-out values of the encoder the residue function is minimised through an iterative process by means of Levenberg – Marquardt algorithm[10]. Final result gives the identified run-out parameters$[e^* \quad \varphi_{ref}^*]$.
5. Finally, the identified run-out parameters can be used for measured angular speed correction.

CONCLUSIONS

The crank angle encoder, used in this research had an identified run-out value of$e^* = 0.07\,mm$. Despite the fact that all possible precautionarymeasures were applied during encoder installation it was very difficult to accomplish near zero run-out condition, mostly due to a specific configuration of the crankshaft free-end shape and its front pulley design. Although the run-out was minimised and through monitored vibration of the encoder, almost unnoticeable, the produced error substantially distorted the information about instantaneous crankshaft angular speed. It is also interesting to note that detected run-out value was below mounting tolerance limits stated in some mounting manuals of the very similar equipment [11].

Kinematic analysis of the crank angle encoder assembly showed that it is possible to derive expressions for the evaluation of the angle encoder measurement errors. The applied CASMA algorithm also proved itself as a useful tool in the process of run-out error parameter identification. Also to have on mind – run-out parameter identification method used strongly relies on the assumption that there is not any significant difference in cylinder overall energy contribution.

It is shown that even a small eccentricity value, as a mounting error, can lead to significant errors in the measurement of the instantaneous angular speed. This is particularly true not only when less sophisticated singular speed measurement devices are used but also in the case of application of single body optical encoders. Special attention should be paid to the mounting and the evaluation of data gathered from the directly mounted encoders by means of secure arm and linkage rod towards the crankcase since the potential error depends not only on mounting eccentricity error but also from other parameters defining the kinematics of crank angle encoder.

REFERENCES

[1] U. Kiencke and R. Eger, Messtechnik: Systemtheorie für Elektrotechniker. Springer, 2008.

[2] P. Leteinturier and J. Benning, “Enhanced Engine Position Acquisition & amp; Treatment,” SAE International, Warrendale, PA, 1999-01-0203, Mar. 1999.

[3] Kiencke U., “Engine misfire detection,” Control Eng. Pract., vol. 7, pp. 203–208, Feb. 1999.

[4] H. Fehrenbach, C. Hohmann, T. Schmidt, W. Schultalbers, and H. Rasche, “Kompensation des Geberradfehlers im Fahrbetrieb,” MTZ, vol. 63, no. 7/8, pp. 588–591, 2002.

[5] H. Fehrenbach, C. Hohmann, T. Schmidt, W. Schultalbers, and H. Rasche, “Bestimmung des Motordrehmoments aus dem Drehzahlsignal,” MTZ, vol. 63, no. 12, pp. 1020–1027, 2002.

[6] H. Fehrenbach and C. Hohmann, “Verfahren zur Bestimmung und Kompensation von Geometriefehlern eines Drehgeberrades,” DE10217560B4.

[7] G. Rämisch, “Modellbasierte Diagnose am Beispiel der Zylinderdrucksensorik von Ottomotoren,” PhD thesis, Universität Kassel, 2009.

[8] L. Miklanek, “Influence of the angle encoder clutch on course of ROHR,” J. KONES Intern. Combust. Engines, vol. 11, no. 3–4, pp. 61–68, 2004.

[9] M. Schmidt, F. Kimmich, H. Straky, and R. Isermann, “Combustion Supervision by Evaluating the Crankshaft Speed and Acceleration,” SAE International, Warrendale, PA, 2000-01-0558, Mar. 2000.

[10] H. Gavin, The Levenberg-Marquardt method for nonlinear least squares. Durham, NC, USA: Department of Civil and Environmental Engineering, Duke University, 2011.

[11] “AVL Operating Instruction In Brief 365C.” AVL List GmbH.

Intentionally blank

A MODEL OF PLANETARY GEAR TRANSMISSION

Ljiljana Veljović[1] *,Vera Nikolić-Stanojević, Dragan Milosavljević , Gordana Bogdanović, Aleksandar Radaković*

UDC: 531.391:62-342

ABSTRACT: In this paper dynamic behaviour of planetary gears with four degrees is analysed by a theoretical approach. Applying the basic principles of analytical mechanics and taking the initial and boundary conditions into consideration, it is possible to obtain the system of equations representing physical meshing process between the two or more gears. The non-linear properties of dynamics which are source of vibrations and noise in the gear transmission may be the caused by small debalances in design realizations of this gears. Using Lagrange's equation, the nonlinear equations of motion are derived. A discrete dynamic model for a planetary gear system is established and the dynamic behaviours of the planetary gear system are investigated. For one planetary gear, eigen fractional modes are obtained and visualization is presented. By using MathCAD the solution is obtained with the time responses computed from the equations of motion.

KEY WORDS: planetary gears, vibrations, fractional order derivative, fractional order eigen mode

MODEL PLANETARNOG PRENOSNIKA

REZIME: U ovom radu se primenom teorijskog pristupa analizira dinamičko ponašanje planetarnog zupčanika sa četiri stepena slobode. Primenom osnovnih principa analitičke mehanike i uzimanjem u obzir početnih i graničnih uslova, moguće je dobiti sistem jednačina koje predstavljaju fizički proces umrežavanja između dva ili više zupčanika. Nelinearna karakteristike dinamike koje su izvor vibracija i buke u zupčastim menjačima mogu biti izazvani malim neuravnoteženostima u procesu izrade i projektovanja ovih zupčanika. Izvedene su nelinearne jednačine kretanja primenom Lagranžeovih jednačina. Diskretni dinamički model planetarni prenosnika je formiran na osnovu ispitivanja dinamičkog ponašanja planetarnog seta zupčanika. Za jedan planetarni prenosnik, sopstveni frakcioni modovi su dobijeni i vizuelno predstavljeni. Rešenja jednačina kretanja u vremenskom domenu dobijena su korišćenjem MathCAD programskog paketa.

KLJUČNE REČI: planetarni zupčanici, vibracije, frakcioni red izvoda i frakcioni red sopstvenog moda.

[1] *Received August 2014, Accepted September 2014, Available on line, June 2015*

Intentionally blank

A MODEL OF PLANETARY GEAR TRANSMISSION

Ljiljana Veljović[1], Vera Nikolić-Stanojević[2], Dragan Milosavljević[3], Gordana Bogdanović[4], Aleksandar Radaković[5]

UDC: 531.391:62-342

INTRODUCTION

Because of its compactness, and high transmission ratios, planetary gears have a great application in modern engineering systems as a replacement for the conventional manual transmission complex. Planetary gears have substantial advantages over parallel shaft drives, including large torque to weight ratio and high efficiency to transfer power. They are widely used for transmissions of automobiles, aircrafts, heavy machinery and marine vehicles. In most high precision reduction of an industrial robot, planetary gears are used in the first stage of gear reducer. Despite the advantages of planetary gears, noise and vibration have been major concerns in their applications.

Generally, a single stage planetary gear-set consists of a sun gear, a ring gear, a carrier, and several planets. Planetary gears possess complicate structure. When modelling planetary gears, both the inertia and the supporting condition should be considered for the sun gear, the ring gear, the carrier and the planets. For this reason, the dynamic analysis of a planetary gear is difficult. Dynamic loads cause damage to the gears, bearings and other elements of the transmission. Precise study of the dynamic behaviour of planetary gear is often a difficult mathematical problem, because there are no adequate models.

Dynamic analyses of the planetary gear system have been investigated by many researchers. First papers on the dynamic behaviour of gears in use, contain a great simplification, such as that all changes have linear character. Experimental studies have shown that this approach is not realistic. The dynamic behaviour of gears is influenced by many factors that cannot be described by linear relationships. The simplest models are found in a number of textbooks used in education in this field. So, the teeth in meshing action can be modelled as an oscillatory system [7], etc. This model consists of concentrated masses connected with elastic and dump element. Each mass represent one gear. For different analysis purposes, there are several modelling choices such as a simple dynamic factor model, compliance tooth model, torsion model, and geared rotor dynamic model, [8]. In order to obtain better results, it is possible to model the elastic element as a nonlinear spring. Natural frequencies and vibration modes are critical parameters that are essential for almost all dynamic investigations. Those parameters may be calculated by using the free vibration

[1] Ljiljana Veljović, Assistant professor, Faculty of Engineering, University of Kragujevac, Sestre Janjić 6, Kragujevac, veljovicljilja@yahoo.co.uk
[2] Vera Nikolic-Stanojevic, Professor emeritus, State University of Novi Pazar, Vuka Karadzica bb, 36300 Novi Pazar, Serbia, veranikolic1@gmail.com
[3] Dragan Milosavljevic, Full professor, Faculty of Engineering, University of Kragujevac, Sestre Janjić 6, Kragujevac, dmilos@kg.ac.rs
[4] Gordana Bogdanovic, Assistant professor, Faculty of Engineering, University of Kragujevac, Sestre Janjić 6, Kragujevac, gocab@kg.ac.rs
[5] Aleksandar Radakovic, Teaching assistant, State University of Novi Pazar, Vuka Karadzica bb, 36300 Novi Pazar, Serbia, sale@1311gmailt.com

analysis. The free vibration properties are very useful for further analyses of planetary gear dynamics, including eigen-sensitivity to design parameters, natural frequency veering, planet mesh phasing, and parametric instabilities from mesh stiffness variations [9].

The dynamic characteristics of the planetary model considering nonlinear time-variable parameters are studied extended it to a three-dimensional model and examined the influence of planet phasing on dynamic response [6]. The planet gears in planetary gear system are fixed at the carrier, so the motion of planets is considered along with the dynamics characteristics of the carrier. In other words, the motion of the planet gears depends on a translation and rotation of the carrier as well as the deflection of the planet gear bearings. Motion of the carrier is considered with the deflections due to the bearings of the planetary gears, because the rigid-body motion of the carrier influences the mesh stiffness between the sun, planetary and ring gears. The revolutions of planets due to the carrier rotation are analysed using polar coordinates [1]. The equations of motion which considered a gyroscopic effect with respect to a rotation are derived also. In recent years, many researchers have used that dynamic model to analyse a planetary gear system.

In the latest research, light fractional order coupling element, is used to describe the dynamic behaviour of gears and set of constitutive relationships, so the fractional calculus can be successfully applied to obtain results [4].

A dynamic model of a planetary gear system in this paper represents a new dynamic model of the fractional order dynamics of the planetary gears with four degrees of freedom. Based on this model, the equations of motion are derived by using Lagrange's equation. The analytical expressions for the corresponding fractional order modes like one frequency eigen vibration modes are obtained.

Applying the Math CAD time integration method to the derived equations, time responses for a planetary gear are calculated. From the computed responses, the dynamic characteristics of the planetary gear system are analysed.

EQUATION OF MOTIONS

Consider the motions of the sun gear, the ring gear, the carrier and the planets gears. It is assumed in this paper that all components of the planetary gear system have the planar motion which is described by translations and rotations.

This model consists of reduced masses of the gear with elastic and damping connections [7]. Contact between two teeth is constructed by standard light element with constitutive stress – strain state relations which can be expressed by fractional order derivatives. In the paper [2] standard light coupling elements of negligible mass in the form of axially stressed rod without bending, with the ability to resist deformation under static and dynamic conditions is analysed in details.

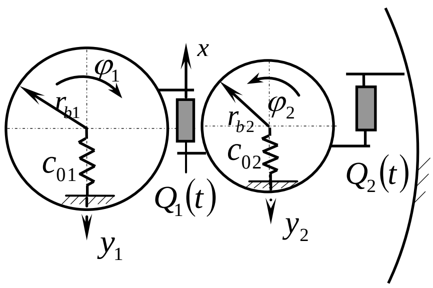

Figure 1 The model of the planetary gear with viscoelastic fractional order tooth coupling

The motion of the sun gear and the ring gear is given by translations that is expressed as y_i, $i=1,2$ and rotations that is expressed as φ_i, $i=1,2$,(Figure 1). The kinetic energy E_K of the planetary stage can be written in a form

$$E_K = E_{K1} + E_{K2}$$

The kinetic energy for the system is represented by:

$$E_K = \frac{1}{2} m_1 \dot{y}_1^2 + \frac{1}{2} J_1 \dot{\varphi}_1^2 + \frac{1}{2} m_2 \dot{y}_2^2 + \frac{1}{2} J_2 \dot{\varphi}_2^2 \qquad (1)$$

Wherem_1 is mass of the sun gear andm_2 is mass of ring gear, $J_1$is mass moment of the inertia of sun gear, J_2 is mass moment of the inertia of ring gear, $\dot{y}_1$ is velocity of mass center of the sun gear and $\dot{y}_2$ is velocity of ring gears mass center; $\dot{\varphi}_1$ is angular velocity of the sun gear and $\dot{\varphi}_2$ is angular velocity of the ring gear.

Sun gear is supported with bearing which is modelled as linear springc_1, but the meshes of sun gear-planet gear and ring gear-planet gear are described by standard light fractional element with stiffness c_{01} and c_{02} . Thus the potential energies of the bearings are:

$$E_p = \frac{1}{2} c_{01} y_1^2 + \frac{1}{2} c_{02} y_2^2 \qquad (2)$$

The potential energy due to gear mesh between the sun gear and the planet gear is

$$E_p = \frac{1}{2} c_1 \left[\left(y_2 + r_{b2} \varphi_2 \right) - \left(y_1 + r_{b1} \varphi_1 \right) \right]^2 \qquad (3)$$

The potential energy due to gear mesh between the ring gear and the planet gear is

$$E_p = \frac{1}{2} c_2 \left(y_2 - r_{b2} \varphi_2 \right)^2 \qquad (4)$$

The equations of motion for the planetary gear are derived from Lagrange's equation given by

$$\frac{d}{dt}\left(\frac{\partial E_K}{\partial \dot{q}_j} \right) - \frac{\partial E_K}{\partial q_j} + \frac{\partial E_P}{\partial q_j} = Q_j^* - \frac{\partial \Phi}{\partial \dot{q}_j}, \quad j = 1,2,\ldots,4 \qquad (5)$$

Where q_j are generalized coordinates (for the given system generalized coordinates are: y_1, y_2, φ_1 and φ_2).

Light standard creep constraint element between sun gear and planet gear is strained for $x_1 = y_2 - y_1 + r_{b2}\varphi_2 - r_{b1}\varphi_1$ and light standard creep constraint element between planet gear and ring gear is strained for $x_2 = y_2 - r_{b2}\varphi_2$.

So, due to the constitutive stress-strain relation of the standard light fractional order coupling elements the restitution forces as a function of elongation of elements are

$$Q_1^* = -c_1 x_1 - c_\alpha D_\alpha^/ [x_1] = -c_1 \left[\left(y_2 + r_{b2}\varphi_2 \right) - \left(y_1 + r_{b1}\varphi_1 \right) \right] - c_\alpha D_\alpha^/ \left[\left(y_2 + r_{b2}\varphi_2 \right) - \left(y_1 + r_{b1}\varphi_1 \right) \right] \qquad (6)$$

$$Q_2^* = -c_2 x_2 - c_\alpha D_\alpha^/\left[x_2\right] = -c_2\left[y_2 - r_{b2}\varphi_2\right] - c_\alpha D_\alpha^/\left[y_2 - r_{b2}\varphi_2\right]$$

Substitution equations (6) into equation (l) the Lagrange equations of motion can be expressed as:

$$m_1\ddot{y}_1 + c_{01}y_1 + c_1\left[(y_1 + r_{b1}\varphi_1) - (y_2 + r_{b2}\varphi_2)\right] = c_\alpha D_\alpha^/\left[(y_2 + r_{b2}\varphi_2) - (y_1 + r_{b1}\varphi_1)\right]$$

$$J_1\ddot{\varphi}_1 + c_1\left[(y_1 + r_{b1}\varphi_1) - (y_2 + r_{b2}\varphi_2)\right]r_{b1} = c_\alpha D_\alpha^/ r_{b1}\left[(y_2 + r_{b2}\varphi_2) - (y_1 + r_{b1}\varphi_1)\right]$$

$$\begin{aligned} &m_2\ddot{y}_2 + c_{02}y_2 + c_1\left[(y_2 + r_{b2}\varphi_2) - (y_1 + r_{b1}\varphi_1)\right] + c_2\left[(y_2 - r_{b2}\varphi_2)\right] = c_\alpha D_\alpha^/\left[(y_1 + r_{b1}\varphi_1) - (y_2 + r_{b2}\varphi_2)\right] - \\ &- c_\alpha D_\alpha^/\left[(y_2 - r_{b2}\varphi_2)\right] \end{aligned} \tag{7}$$

$$\begin{aligned} &J_2\ddot{\varphi}_2 + c_1\left[(y_2 + r_{b2}\varphi_2) - (y_1 + r_{b1}\varphi_1)\right]r_{b2} + c_2\left[r_{b2}\varphi_2 - y_2\right]r_{b2} = c_\alpha D_\alpha^/\left[(y_1 + r_{b1}\varphi_1) - (y_2 + r_{b2}\varphi_2)\right] + \\ &+ c_\alpha D_\alpha^/\left[(y_2 - r_{b2}\varphi_2)\right] \end{aligned}$$

The matrix form of equations is well known as:

$$\mathbf{M}\{\ddot{q}\} + \mathbf{C}\{q\} = Q_j^* - \frac{\partial\Phi}{\partial\dot{q}_j}, \quad j = 1,2,\ldots,4 \tag{8}$$

with matrix $\mathbf{M}$ as diagonal inertia matrix in a form:

$$\mathbf{M} = \begin{bmatrix} m_1 & & & \\ & J_1 & & \\ & & m_2 & \\ & & & J_2 \end{bmatrix} \tag{9}$$

and the matrix $\mathbf{C}$ as stiffness matrix that is in a form:

$$\mathbf{C} = \begin{bmatrix} c_{01} + c_1 & c_1 r_{b1} & -c_1 & -c_1 r_{b2} \\ c_1 r_{b1} & c_1 r_{b1}^2 & -c_1 r_{b1} & -c_1 r_{b1} r_{b2} \\ -c_1 & -c_1 r_{b1} & c_{02} + c_1 + c_2 & (c_1 - c_2) r_{b2} \\ -c_1 r_{b2} & -c_1 r_{b1} r_{b2} & (c_1 - c_2) r_{b2} & (c_1 + c_2) r_{b2}^2 \end{bmatrix} \tag{10}$$

MODAL ANALYSIS

Eigenvalue problem

The proposed solutions are in the form:

$$\{q\} = \{A\}\cos(\omega t + \varepsilon) \tag{11}$$

and it can be written as:

$$(\mathbf{C} - \lambda\mathbf{M})\{q\} = 0 \tag{12}$$

The matrix on the left side is singular in aim to obtain non-trivial solutions. It follows that the determinant of the matrix mast be equal to 0, so:

$$\begin{bmatrix} (c_{01}+c_1)-\lambda m_1 & c_1 r_{b1} & -c_1 & -c_1 r_{b2} \\ c_1 r_{b1} & (c_1 r_{b1}^2)-\lambda J_1 & -c_1 r_{b1} & -c_1 r_{b1} r_{b2} \\ -c_1 & -c_1 r_{b1} & (c_{02}+c_1+c_2)-\lambda m_2 & (c_1-c_2) r_{b2} \\ -c_1 r_{b2} & -c_1 r_{b1} r_{b2} & (c_1-c_2) r_{b2} & ((c_1+c_2) r_{b2}^2)-\lambda J_2 \end{bmatrix} = 0 \qquad (13)$$

Solving this determinant four eigen circular frequencies $\omega_j = \sqrt{\lambda_j}$, $j = 1,2,3,4$, can be obtained.

The solution of basic linear differential equation is:

$$\{q(t)\} = \mathbf{R}\{C_s \cos(\omega_s t + \varepsilon_s)\} \qquad (14)$$

where $\mathbf{R}$ is modal matrix defined by the corresponding cofactors and $\xi_s = C_s \cos(\omega_s t + \varepsilon_s)$, $s = 1,2,3,4$ are main coordinates of the linear system. The system of the fractional differential equations (7) can be transformed in the form [2]:

$$\ddot{\xi}_s + \omega_s^2 \xi_s = -\omega_{\alpha s}^2 D_\alpha^{/}[\xi_s], \; s = 1,2,3,4 \qquad (15)$$

Using the approach presented in [2] the solution of the basis system (7) can be expressed in the following form:

$$\begin{aligned} \xi_s(t) = {} & \xi_{0s} \sum_{k=0}^{\infty} (-1)^k \omega_{\alpha s}^{2k} t^{2k} \sum_{j=0}^{k} \binom{k}{j} \frac{(\mp 1)^j \omega_{\alpha s}^{2j} t^{-\alpha j}}{\omega_s^{2j} \Gamma(2k+1-\alpha j)} + \\ & + \dot{\xi}_{0s} \sum_{k=0}^{\infty} (-1)^k \omega_{\alpha s}^{2k} t^{2k+1} \sum_{j=0}^{k} \binom{k}{j} \frac{(\mp 1)^j \omega_{\alpha s}^{-2j} t^{-\alpha j}}{\omega_s^{2j} \Gamma(2k+2-\alpha j)}, \;, s = 1,2,3,4 \end{aligned} \qquad (16)$$

Where $\xi_s(0) = \xi_{0s}$ and $\dot{\xi}_s(0) = \dot{\xi}_{0s}$ are initial values of main coordinates defined by initial conditions.

Computation observation

Eigen solutions of a sample system with four degrees of freedom are evaluated numerically to expose the modal properties.

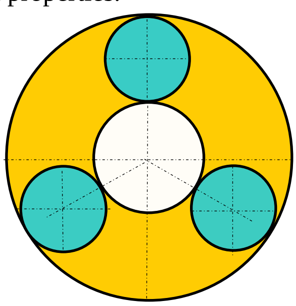

Figure 2 The initial position of planet gear

For the Sun base radius r_{b1}=24 mm, Planet base radius r_{b2}=16 mm, Radial bearing stiffnesses $c_{01} = 0.5x10^9$ N/m and $c_{02} = 0.5x10^9$ N/m, Stiffness of teeth $c_1 = 2.91x10^8$ N/m and c_2= $1.81x10^8$ N/m, Mass m_1= 0.3 kg, m_2= 0.3 kg, Rotational inertia, J_1=$10x10^{-3}$ and J_2=$100x10^{-6}$ kgm^2 some So,

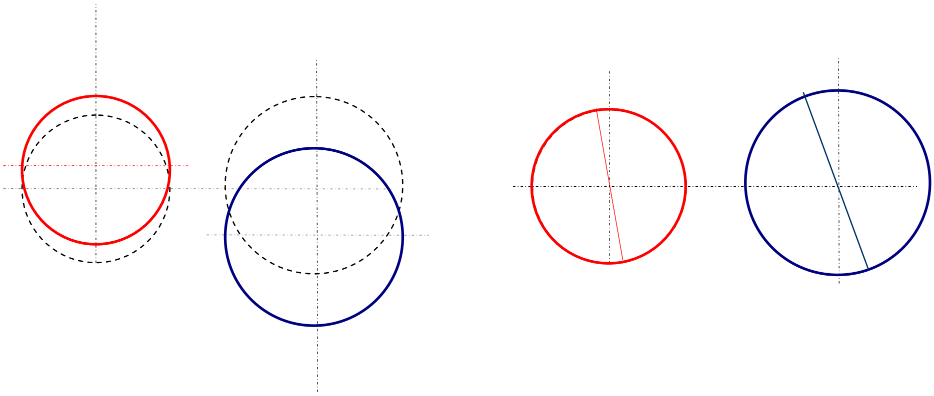

Figure 3 Translational (a) and angular (b) displacement modes (215,564 Hz) mesh of sun-gear planet gear defined in [8]

For one planetary gear, eigen fractional modes are obtained and visualization is presented on Figure 3 by using MathCAD .

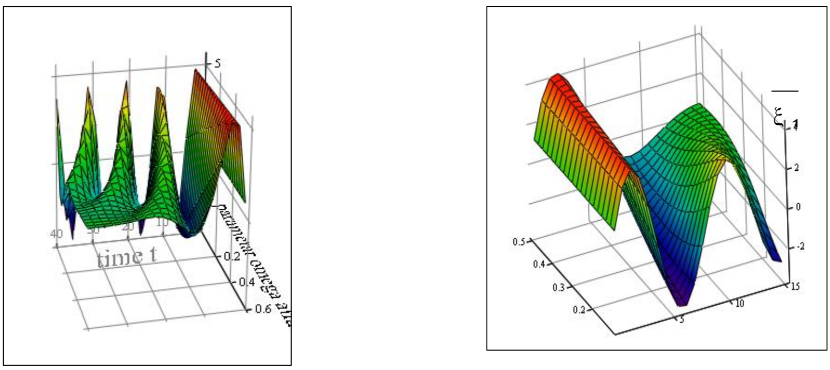

s

S

Figure 4 First main coordinates defined by initial conditions; $\xi_s(0) = \xi_{0s}$ *and* $\dot{\xi}_s(0) = \dot{\xi}_{0s}$

The first main coordinate is decreasing and increasing for changing of parameter α

.

DYNAMIC RESPONSE ANALYSIS

The mechanical systems presented in this paper contain several simplifications. The planetary gear system is modelled as a mass-less shaft, bearings are assumed to be linear as linear elastic springs and the gears are assumed to be rigid.

However, the results in paper [4] and paper [5] indicate that the models with these simplifications acceptably predict the system characteristics.

Dynamic responses of the planetary gear system are computed from equation (16), using the Math CAD software.

Based on equation (18), the first normal mode corresponds to both masses moving in the opposite direction while angular displacements are in the same direction.

The numerical simulations indicate that the first, second and third fourth eigen frequencies are different from zero but the fourth eigen frequency is equal to zero for the presented values. Also, one can see 4-5 peaks of first main coordinate presented on Figure 4. The first main coordinate is decreasing and increasing unbalance for an increase of parameter α (Figure 4a). According to Figure 4b one can see that the first main coordinate is changing with increasing of parameter ω_α . Parameters α and ω_α are parameters that define the derivation of fractional order differential operator [3].

CONCLUSIONS

The dynamic characteristics of planetary gear system are analysed considering the motion of carrier which influences the translation and rotation motions of the planetary gears. The equations of motion for the planetary gear system are derived by applying the Lagrange equation. Based upon the derived equations, the time responses are computed using the Math CAD. The dynamic behaviours of the planetary gear system are investigated with the time responses computed from the equations of motion. In addition, the motions of the components are also studied when they are in a steady state. The new model of the fractional order dynamic planetary gear here presented can be applied to study the real behaviour of the planetary gear. With this simple model, it is possible to research the nonlinear dynamics of the planetary gear and nonlinear phenomena in free and forced dynamics. The model is suitable to explain source of vibrations and big noise, as well as no stability in planetary gear.

In this paper a new method is used for the obtaining of the eigen values and for analysis results by MATCAD software.

ACKNOWLEDGMENTS

Parts of this research were supported by the Ministry of Sciences of Republic Serbia through Mathematical Institute SANU Belgrade Grants No. ON 174001 “Dynamics of hybrid systems with complex structures. Mechanics of materials” and also through the Faculty of Mechanical Engineering University of Niš and the State University of Novi Pazar.

REFERENCES

[1] Cheon-Jae, B., Parker, G. R.: “Analytical Solution for the Nonlinear Dynamics of Planetary Gears”, Journal of Computational and Nonlinear Dynamics APRIL 2011, Vol. 6 / 021007-1 - 021007-15., 2011,New York City,p. 298-319

[2] Goroško, O. A. i Hedrih (Stevanović), K.: “Analitička dinamika (mehanika) diskretnih naslednih sistema, (Analytical Dynamics (Mechanics) of Discrete Hereditary Systems)”, Monograph, 2001, University of Niš, p. 426

[3] Hedrih K.: “Dynamics of multi-pendulum systems with fractional order creep elements”, Journal of Theoretical andApplied Mechanics, vol. 46, no. 3, 2008, pp. 483–509

[4] Hedrih (Stevanovic), K., Nikolic-Stanojevic, V.: “A model of gear transmission fractional order system dynamics”. Mathematical Problems in Engineering from: http://www.hindawi.com/journals/mpe/ aip972873.html accesed on 2010-05-06.

[5] Lin, J., Parker, G.R.: ‘‘Analytical characterization of the unique properties of planetary gear free vibration. Transactions of the ASME’’, vol. 121, 1999,New York City,p. 316-321.

[6] Nikolic, V.: ’’Machine elements, theory, calculation, examples’’, Faculty of Mechanical Engineering, Prizma, 2004. Kragujevac, p. 671

[7] Nikolic, V. : ’’Mechanical analysis of gears’’, Faculty of Mechanical Engineering, Cimpes, 1999, Kragujevac, p. 189

[8] Nikolic-Stanojevic V., Veljovic Lj., Dolicanin C.: ’’A new Model of the Fractional order Dynamics of the Planetary gears’’, Mathematical Problems in Engineering, Volume, 2013 Article ID 932150, 14 pages http://dx.doi.org/10.1155/2013/932150

[9] Vinayak, H., Singh, R.: ’’Multi-body dynamics and modal analysis of compliant gear bodies’’, Journal of Sound and Vibration, Vol. 210, no. 2, 1998, Great Britain, p. 171-214.

DYNAMIC MODEL OF CYCLOIDAL SPEED REDUCER

Mirko Blagojević[1], Zorica Đorđević, Miloš Matejić, Nenad Kostić, Nenad Petrović

UDC: 621.833.058:[519.6]

ABSTRACT: Cycloidal speed reducer is a very complex mechanical system and for studying its dynamic behaviour must be considered all its specifics. On the level of internal dynamic forces very big impact have: manufacturing errors of cycloid disc and other elements of reducer, assembly errors, unequal load distribution, ... On the basis of the models of external and internal gear trains, a dynamic model of a single - stage cycloidal speed reducer is developed in the paper. It is assumed that the values of the stiffness are constant and the excitation force time-variable function. The values of displacement, velocity, and dynamic force for single meshing are presented in this paper. The greatest impact on the dynamic force value has the coefficient of damping and coefficient of stiffness between cycloid disc and the ring gear.

KEY WORDS: cycloidal speed reducer, cycloid disc, dynamic model, dynamic force

DINAMIČKI MODEL CIKLOIDNOG REDUKTORA BRZINE

REZIME: Cikloidni reduktor brzine je veoma složeni mehanički sistem i za analizu njegovog dinamičkog ponašanja moraju se uzeti u obzir sve specifičnosti. Na nivou unutrašnjih dinamičkih sila značajan uticaj imaju: greške u proizvodnji cikloidnog diska i drugih elemenata reduktora, greške sklopa, neravnomerna raspodela opterećenja i drugo. Na osnovu modela spoljašnjih i unutrašnjih prenosnika, dinamički model jednog cikloidnog reduktora brzine razvijen je u ovom radu. Pretpostavljeno je da su vrednosti krutosti konstantne i da je sila pobuda vremenski zavisna funkcija. Vrednosti pomeranja, brzine, i dinamičke sile za jedan tip mreže su prikazani u ovom radu. Najveći uticaj na vrednost dinamičke sile ima koeficijent prigušenja i koeficijent krutosti između cikloidnog diska i prstenastoga zupčanika.

KLJUČNE REČI: cikloidni reduktor brzine, cikloidni disk, dinamički model, dinamička sila

[1] *Received September 2014, Accepted October 2014, Available on line June 2015*

Intentionally blank

DYNAMIC MODEL OF CYCLOIDAL SPEED REDUCER

Mirko Blagojević[1], Zorica Đorđević[2], Miloš Matejić[3], Nenad Kostić[4], Nenad Petrović[5]

UDC:621.833.058:[519.6]

INTRODUCTION

Thanks to the application of internal spur gears, planetary gearboxes are characterized by extreme compactness of the structure, high transmission ratios, as well as a good balance of the dynamic forces. Consequences of the smaller gear dimensions used in planetary speed reducer are mainly smaller rotational speeds and the sliding and rolling speed on the teeth. As a result, the dynamic load sand vibrations in the elements of the planetary gear trains are less. The sliding and rolling speeds on the teeth in the planetary gear are lower by approximately 30% to 40% compared to conventional speed reducer with parallel axes. Also, it should be noted significantly less rotating mass (up 75%), lower moment of inertia, the less impact force when starting and stopping gear, [4, 17].

Cycloidal speed reducer belongs to a group of modern planetary gear. Thanks to its good working characteristics (large gear ratio, long and reliable service life, compact design, high efficiency, low vibration, low noise, ...), cycloidal speed reducers have very widely application in modern industry.

In order to describe the dynamic behaviour of the cycloidal speed reducer, the first were analysed well known dynamic models of planetary gears classical concepts. The dynamic models of planetary speed reducers are presented in papers [9, 10]. The same author (*Kahraman*) with a group of co-authors analysed the influence of the ring gear rim thickness on planetary gear set behaviour, [11, 12]. Determination of gear mesh stiffness and internal dynamic forces at planetary gear drives is presented in papers [1, 2, 3, 15]. The elasto-dynamic model of internalgear planetary transmissions is described in paper [19]. Determination of planetary gear natural frequencies and vibration modes is presented in papers [7, 14].

In the papers [5, 13, 17] the various procedures for calculating of the cycloidal speed reducer efficiency have presented. Determination of stress and strain state of cycloidal speed reducer elements using the FEM in static and dynamic conditions is presented in papers [6, 8, 18]. The procedure for torsion stiffness calculation of cycloidal speed reducer is defined in paper [16].

A dynamic model of a single - stage cycloidal speed reducer is developed in this paper.

[1]*Mirko Blagojević, Associate Professor, Faculty of Engineering, University of Kragujevac, Sestre Janjić 6, Kragujevac, mirkob@kg.ac.rs*
[2]*Zorica Đorđević, Associate Professor, Faculty of Engineering, University of Kragujevac, Sestre Janjić 6, Kragujevac, zoricadj@kg.ac.rs*
[3]*Miloš Matejić, Ph.D student, Faculty of Engineering, University of Kragujevac, Sestre Janjić 6, Kragujevac, mmatejic@kg.ac.rs*
[4]*Nenad Kostić, Ph.D student, Faculty of Engineering, University of Kragujevac, Sestre Janjić 6, Kragujevac, nkostic@kg.ac.rs*
[5]*Nenad Petrović, Ph.D student, Faculty of Engineering, University of Kragujevac, Sestre Janjić 6, Kragujevac, npetrovic@kg.ac.rs*

DYNAMIC MODEL OF ONE - STAGE CYCLOIDAL SPEED REDUCER

The main generators of internal dynamic forces in gear drives are: changes of deformations in meshing process, collisions of teeth in the meshing process, profile shape deviations, tooth wear, etc. Cycloidal speed reducer is a very complex mechanical system and for studying its dynamic behavior it is necessary to take into accounts all of its peculiarities. The greatest impact on the internal dynamic forces at cycloidal speed reducer have: errors that occur during the production of cycloid disc's teeth, as well as other elements of cycloidal speed reducer, unequal distribution of load at cycloid disc teeth as well as at stationary central gear rollers and output rollers, elastic deformations of case and other elements,…

On the basis of a very careful analysis of dynamic models of external involute tooth gearing, as well as dynamic model of planetary gear trains, the dynamic model of single - stage cycloidal speed reducer was developed in this paper. This model is presented in Figure 1.

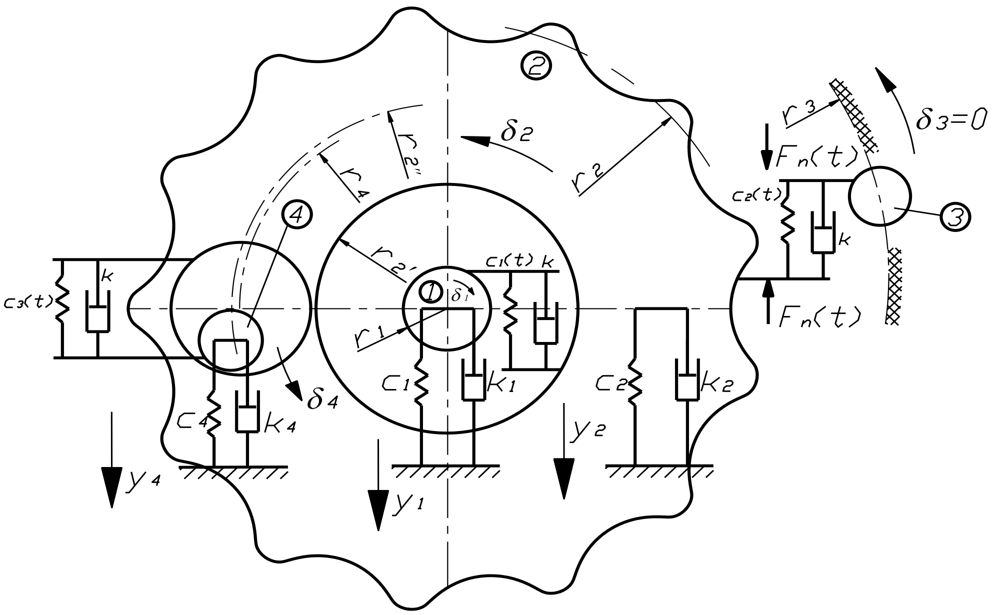

Figure 1 Dynamic model of a single-stage cycloidal speed reducer (1-input shaft with the eccentric cam, 2-cycloid disc, 3-stationary central gear roller, output roller)

The geometric dimensions from figure 1 are:

r_1 – external radius of the eccentric cam,
r_2 – radius of the pitch circle of the cycloid disc,
$r_2^{`}$– radius of the central hole of the cycloid disc,
$r_2^{``}$ – radius of the cycloid disc circle with the holes for the output rollers,
r_3 – radius of the pitch circle of the stationary central gear,
r_4 – radius of the output shaft flange with the holes for corresponding rollers.

The cycloidal speed reducer elements are connected in their supports in the following way:

- Input shaft with eccentric cam: elastic connect of the stiffness c_1 and a damper with the coefficient of damping k_1,
- Cycloid disc: elastic connection of the stiffness c_2 and a damper with coefficient of damping k_2,
- Stationary central gear roller: elastic connection of the stiffness c_3 and a damper with the coefficient of damping k_3,
- Output roller: elastic connection of the stiffness c_4 and a damper with the coefficient of damping k_4.

The contacts between the corresponding elements of the cycloidal speed reducer are described in the following way:

- Input shaft with eccentric cam – cycloid disc: elastic connection of the variable stiffness $c_1(t)$ and damper with the coefficient of damping k,
- Cycloid disc – stationary central gear roller: elastic connection of the variable stiffness $c_2(t)$ and a damper with the coefficient of damping k,
- Cycloid disc – output roller: elastic connection with the variable coefficient of stiffness $c_3(t)$ and a damper with the coefficient of damping k.

The excitation force $F_n(t)$ occurs in the contact between the cycloid disc tooth and the stationary central gear roller. The excitation force is calculated using the following expression, [1, 2, 3]:

$$F_n(t) = c \cdot w(t) \cdot b \, , \tag{1}$$

where:

c - connected teeth stiffness,

w(t) - deformation of the cycloid disc tooth,

b - cycloid disc width.

For as much as deformation`s magnitude periodical time`s function, the same case is for excitation force. The total displacement x in the contact between the cycloid disc tooth and the stationary central gear roller can be expressed as follows:

$$x = r_2 \cdot \delta_2 - y_2 \, , \tag{2}$$

The result of the excitation force action is a dynamic force which loads the cycloid disc teeth and the stationary central gear rollers:

$$F_e = c \cdot x + b \cdot \dot{x} \, , \tag{3}$$

The kinetic system energy is:

$$E_k = \frac{1}{2} m_1 \cdot \dot{y}_1^2 + \frac{1}{2} J_1 \cdot \dot{\delta}_1^2 + \frac{1}{2} m_2 \cdot \dot{y}_2^2 + \frac{1}{2} J_2 \cdot \dot{\delta}_2^2 + \frac{1}{2} m_4 \cdot \dot{y}_4^2 + \frac{1}{2} J_4 \cdot \dot{\delta}_4^2 \, , \tag{4}$$

$$E_p = \frac{1}{2}c_1 \cdot y_1^2 + \frac{1}{2}c_2 \cdot y_2^2 + \frac{1}{2}c_4 \cdot y_4^2 + \frac{1}{2}c_1(t) \cdot \left[\left(y_2 - r_2' \cdot \delta_2\right) - \left(y_1 + r_1 \cdot \delta_1\right)\right]^2 + \frac{1}{2}c_2(t) \cdot \left[\left(y_2 - r_2 \cdot \delta_2\right)\right]^2 + \\ + \frac{1}{2}c_3(t) \cdot \left[\left(y_4 + r_4 \cdot \delta_4\right) - \left(y_2 + r_2'' \cdot \delta_2\right)\right]^2 \tag{5}$$

The dissipation system function is:

$$\Phi = \frac{1}{2}k_1 \cdot \dot{y}_1^2 + \frac{1}{2}k_2 \cdot \dot{y}_2^2 + \frac{1}{2}k_4 \cdot \dot{y}_4^2 + \frac{1}{2}k \cdot \left[\left(\dot{y}_2 - r_2' \cdot \dot{\delta}_2\right) - \left(\dot{y}_1 + r_1 \cdot \dot{\delta}_1\right)\right]^2 + \frac{1}{2}k \cdot \left[\left(\dot{y}_2 - r_2 \cdot \dot{\delta}_2\right)\right]^2 + \\ + \frac{1}{2}k \cdot \left[\left(\dot{y}_4 + r_4 \cdot \dot{\delta}_4\right) - \left(\dot{y}_2 + r_2'' \cdot \dot{\delta}_2\right)\right]^2 \tag{6}$$

The virtual work of the conservative forces is:

$$\partial A = F_n(t) \cdot r_2 \cdot \partial \delta_2 , \tag{7}$$

The conservative force is:

$$Q_{\delta_2} = F_n(t) \cdot r_2 , \tag{8}$$

The signs m_1, m_2 and m_3 stand for masses of correspondent elements, and J_1, J_2 and J_3 stand for a rectangular moment of inertia of the same elements.

Stiffnesses in the corresponding contacts and the dynamic force are variable time functions. However, in order to enable the analysis of influence of deviation of geometric dimensions, it is adopted that the mentioned stiffnesses are constant and equal to some average values, and the excitation force stay a variable time function.

$$\begin{aligned} c_1(t) &= c_{01} = const. \\ c_2(t) &= c_{02} = const. \\ c_3(t) &= c_{03} = const. , \end{aligned} \tag{9}$$

The differential equation of the system motion in matrix form is:

$$\begin{bmatrix} J_1 & 0 & 0 & 0 & 0 & 0 \\ 0 & m_1 & 0 & 0 & 0 & 0 \\ 0 & 0 & J_2 & 0 & 0 & 0 \\ 0 & 0 & 0 & m_2 & 0 & 0 \\ 0 & 0 & 0 & 0 & J_4 & 0 \\ 0 & 0 & 0 & 0 & 0 & m_4 \end{bmatrix} \begin{Bmatrix} \ddot{\delta}_1 \\ \ddot{y}_1 \\ \ddot{\delta}_2 \\ \ddot{y}_2 \\ \ddot{\delta}_4 \\ \ddot{y}_4 \end{Bmatrix} + \begin{bmatrix} k \cdot r_1^2 & k \cdot r_1 & k \cdot r_1 \cdot r_2' & -k \cdot r_1 & 0 & 0 \\ k \cdot r_1 & k_1 + k & k \cdot r_2' & -k & 0 & 0 \\ k \cdot r_1 \cdot r_2' & k \cdot r_2' & k \cdot \left[\left(r_2'\right)^2 + \left(r_2''\right)^2 + r_2^2\right] & k \cdot \left(-r_2' + r_2'' - r_2\right) & -k \cdot r_4 \cdot r_2'' & -k \cdot r_2'' \\ k \cdot r_1 & k & k \cdot \left(r_2' + r_2'' + r_2\right) & k_2 - k & k \cdot r_4 & -k \\ 0 & 0 & -k \cdot r_4 \cdot r_2'' & -k \cdot r_4 & k \cdot r_4^2 & k \cdot r_4 \\ 0 & 0 & -k \cdot r_2'' & -k & k \cdot r_4 & k + k_4 \end{bmatrix} \begin{Bmatrix} \dot{\delta}_1 \\ \dot{y}_1 \\ \dot{\delta}_2 \\ \dot{y}_2 \\ \dot{\delta}_4 \\ \dot{y}_4 \end{Bmatrix} + \\ + \begin{bmatrix} c_{01} \cdot r_1^2 & c_{01} \cdot r_1 & c_{01} \cdot r_1 \cdot r_2' & -c_{01} \cdot r_1 & 0 & 0 \\ c_{01} \cdot r_1 & c_1 + c_{01} & c_{01} \cdot r_2' & -c_{01} & 0 & 0 \\ c_{01} \cdot r_1 \cdot r_2' & c_{01} \cdot r_2' & c_{01} \cdot \left(r_2'\right)^2 + c_{02} \cdot r_2^2 + c_{03} \cdot \left(r_2''\right)^2 & -c_{01} \cdot r_2' + c_{03} \cdot r_2'' - c_{02} \cdot r_2 & -c_{03} \cdot r_4 \cdot r_2'' & -c_{03} \cdot r_2'' \\ c_{01} \cdot r_1 & c_{01} & c_{01} \cdot r_2' + c_{03} \cdot r_2'' + c_{02} \cdot r_2 & -c_{01} + c_2 - c_{02} + c_{03} & -c_{03} \cdot r_4 & -c_{03} \\ 0 & 0 & -c_{03} \cdot r_4 \cdot r_2'' & -c_{03} \cdot r_4 & c_{03} \cdot r_4^2 & c_{03} \cdot r_4 \\ 0 & 0 & -c_{03} \cdot r_2'' & -c_{03} & c_{03} \cdot r_4 & c_{03} \end{bmatrix} \begin{Bmatrix} \delta_1 \\ y_1 \\ \delta_2 \\ y_2 \\ \delta_4 \\ y_4 \end{Bmatrix} = \begin{Bmatrix} 0 \\ 0 \\ F_n(t) \cdot r_2 \\ 0 \\ 0 \\ 0 \end{Bmatrix} \tag{10}$$

DYNAMIC BEHAVIOUR OF ONE CONCRETE ONE - STAGE CYCLOIDAL SPEED REDUCER

The differential equation of the system motion was solved using MATLAB - SIMULINK for one concrete one - stage cycloidal speed reducer with following working parameters:

- Input power: P_{in} = 0,25 kW;
- Input rotations per minute: n_{in} = 1390 min^{-1};
- Reduction ratio: u = 11.

The input system parameter is the excitation force $F_n(t)$, and the output parameters are: total displacement (x) in the point of contact between a cycloid disc tooth and a stationary central gear roller, the adequate velocity ($\dot{x}$) and the dynamic force F_e.

The values of the coefficients of damping as well as adequate stiffnesses are adopted from literature [1, 2, 3, 15]:

k = 5500 Ns/m, k_1 = 2700 Ns/m, k_2 = 200 Ns/m, k_3 = 1800 Ns/m, k_4 = 1000 Ns/m, $c_{01} = 1,4\cdot10^8$ N/mm, $c_{02} = 1,5\cdot10^7$ N/mm, $c_{03} = 1,6\cdot10^8$ N/mm, $c_1 = 1,9\cdot10^9$ N/mm, $c_2 = 1,7\cdot10^8$ N/mm, $c_3 = 2,1\cdot10^9$ N/mm, $c_4 = 1,6\cdot10^8$ N/mm.

The masses of elements, the rectangular moments of inertia and the adequate radii have the following values: m_1 = 0,17 kg, m_2 = 0,74 kg, m_4 = 0,70 kg, J_1 = 26 $kgmm^2$, J_2 =1422,3 $kgmm^2$, J_4 = 762,5 $kgmm^2$, r_1 = 17,5 mm, r_2 = 62 mm, r_2' = 20 mm, r_2'' = 39 mm, r_4 = 39 mm.

Diagram of excitation force is presented in Figure 2, and the results of calculation for total displacement, velocity and dynamic force are presented in Figures 3,4 and 5.

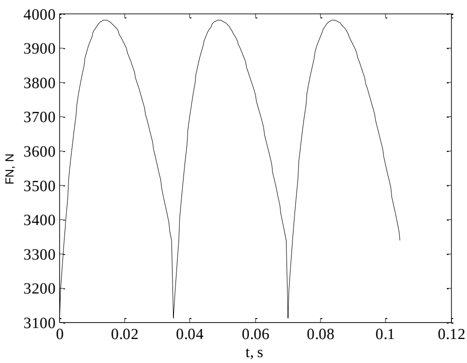

Figure 2 Diagram of excitation force $F_n(t)$

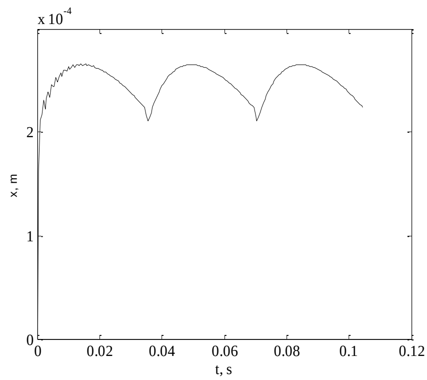

Figure 3 Diagram of the total displacement x

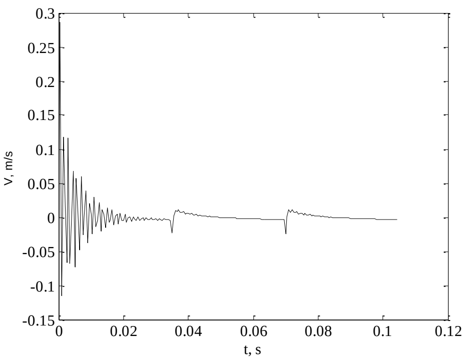

Figure 4 Diagram of the velocity $\dot{x}$

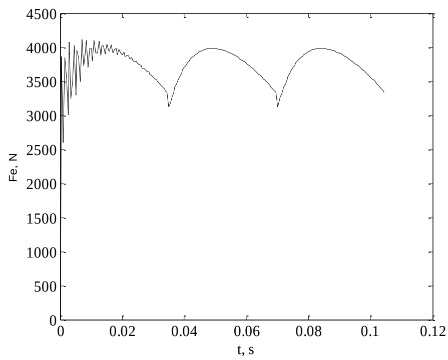

Figure 5 Diagram of the dynamic force Fe

The presented results refer to the most critical case - the case of single meshing (one cycloid disc tooth and one stationary central gear roller are in the contact).

CONCLUSIONS

When the values for the coefficients of damping and adequate stiffnesses are selected from a recommended range, vibrations with damping in time disappear very quickly and only forced vibrations remain.

Forasmuch as the excitation force is a periodical time function, the same goes for the other parameters (total displacement, velocity and the dynamic force).

The biggest influence on dynamic behaviour of one - stage cycloid speed reducer has the coefficient of the damping during the contact between the cycloid disc tooth and the stationary central gear roller.

REFERENCES

[1] Batinic, V.: "Determination of Gear Mesh Stifness in Planetary Gearing", Military Technical Courir, Vol.56, No.2, 2008, pp. 227-236.

[2] Batinic, V.: "Dynamic Stability of Planetary Gear Drives", International Conference Research and Development of Mechanical Elements and Systems - IRMES, 2008, Beograd, Serbia,pp. 539-544.

[3] Batinic, V.: "Internal Dynamic Forces at Planetary Gear Drives", Scientific Technical Review, Vol.LI, No.3, 2001, pp. 43-48.

[4] Blagojevic, M., Marjanovic, N., Djordjevic, Z., Stojanovic, B., Disic, A.: "A New Design of a Two-Stage Cycloidal Speed Reducer", Journal of Mechanical Design, Vol.133, No.8, 2011, pp. 085001-1-085001-7.

[5] Blagojevic, M., Kocic, M., Marjanovic, N., Stojanovic, B., Djordjevic, Z., Ivanovic, L., Marjanovic, V.: "Influence of the Friction on the Cycloidal Speed Reducer Efficiency", Journal of the Balkan Tribological Association, Vol.18, No.2, 2012, pp. 217-227.

[6] Blagojevic, M., Marjanovic, N., Djordjevic, Z., Stojanovic, B., Marjanovic, V., Vujanac, R., Disic, A.: "Numerical and Experimental Analysis of the Cycloid Sisc Stress State", Technical Gazette, Vol.21, No.2, 2014, pp. 377-382.

[7] Guo, Y., Parker, R.: "Sensitivity of General Compound Planetary Gear Natural Frequencies and Vibration Modes to Modal Parameters", Journal of Vibration and Acoustics, Vol.132, No.1, 2010, pp. 011006-1-011006-13.

[8] Hsieh, C.F.: "The Effect on Dynamic of Using a New Transmission Design for Eccentric Speed Reducer", Mechanism and Machine Theory, Vol. 80, 2014, pp. 1-16.

[9] Kahraman, A.: "Load Sharing Characteristics of Planetary Transmissions", Mechanism and Machine Theory, Vol.29, No.8, 1994, pp. 1151-1165.

[10] Kahraman, A.: "Free Torsional Vibration Characteristics of Compound Planetary Gear Sets", Mechanism and Machine Theory, Vol.36, No.8, 2001, pp. 953-971.

[11] Kahraman, A., Kharazi, A.A., Umrani, M.: "A Deformable Body Dynamic Analysis of Planetary Gears With Thin Rims", Journal of Sound and Vibration, Vol.262, No.3, 2003, pp. 752-768.

[12] Kahraman, A., Ligata, H., Singh, A.: "Influence of Ring Gear Rim Thickness on Planetary Gear Set Behaviour", Journal of Mechanical Design, Vol.132, No.2, 2010, pp. 021002-1-021002-8.

[13] Kosse, V.: "Using Hysteresis Loop and Torsional Shock Loading to Asses Damping and Efficiency of Cyclodrive", 14th International Congress on Sound and Vibration, 2007., Cairns, Australia, pp. 1-8.

[14] Lin, J., Parker, R.G.: "Sensitivity of Planetary Gear Natural Frequencies and Vibration Modes to Model Parameters", Journal of Sound and Vibration, Vol.228, No.1, 1999, pp. 109-128.

[15] Lin, J., Parker, R.G.: "Planetary Gear Parametric Instability Caused by Mesh Stiffness Variation", Journal of Sound and Vibration, Vol.249, No.1, 2002, pp. 129-145.

[16] Liu, J., Matsumura, S., Chen, B., Houjoh, H.: "Torsional Stifness Calculation of Double-Enveloping Cycloid Drive", Journal of Advanced Mechanical Design, Systems, and Manufacturing, Vol.6, No.1, 2012, pp. 2-14.

[17] Malhotra, S.K., Parameswaran, M.A.: "Analysis of a Cycloid Speed Reducer", Mechanism and Machine Theory, Vol.18, No.6, 1983, pp. 491-499.

[18] Thube, S.V., Bobak, T.R.: "Dynamic Analysis of a Cycloidal Gearbox Using Finite Element Method", AGMA Technical Paper, 2012, pp. 1-13.

[19] Yang, J, Zhang, C.: "Elasto-dynamics of Internal Gear Planetary Transmissions", Mechanism and Machine Theory, Vol.40, No.10, 2005, pp. 1107-1125

NOTIFICATION TO AUTHORS

The Journal MVM publishes original papers which have not been previously published in other journals. This is responsibility of the author. The authors agree that the copyright for their article is transferred to the publisher when the article is accepted for publication.

The language of the Journal is English.

Journal ***Mobility & Vehicles Mechanics*** is at the SSCI list.

All submitted manuscripts will be reviewed. Entire correspondence will be performed with the first-named author.

Authors will be notified of acceptance of their manuscripts, if their manuscripts are adopted.

INSTRUCTIONS TO AUTHORS AS REGARDS THE TECHNICAL ARRANGEMENTS OF MANUSCRIPTS:

Abstract is a separate Word document, "*First author family name_ABSTRACT.doc*". Native authors should write the abstract in both languages (Serbian and English). The abstracts of foreign authors will be translated in Serbian.

This document should include the following: 1) author's name, affiliation and title, the first named author's address and e-mail – for correspondence, 2) working title of the paper, 3) abstract containing no more then 100 words, 4) abstract containing no more than 5 key words.

The manuscript is the separate file, „*First author family name_Paper.doc*" which includes appendices and figures involved within the text. At the end of the paper, a reference list and eventual acknowledgements should be given. References to published literature should be quoted in the text brackets and grouped together at the end of the paper in numerical order.

Paper size: Max 16 pages of B5 format, excluding abstract
Text processor: Microsoft Word
Margins: left/right: mirror margin, inside: 2.5 cm, outside: 2 cm, top: 2.5 cm, bottom: 2 cm
Font: Times New Roman, 10 pt
Paper title: Uppercase, bold, 11 pt
Chapter title: Uppercase, bold, 10 pt
Subchapter title: Lowercase, bold, 10 pt
Table and chart width: max 125 mm
Figure and table title: Figure _ (Table _): Times New Roman, italic 10 pt

Manuscript submission: application should be sent to the following e-mail:

mvm@kg.ac.rs ; lukicj@kg.ac.rs
or posted to address of the Journal:
University of Kragujevac – Faculty of Engineering
International Journal M V M
Sestre Janjić 6, 34000 Kragujevac, Serbia

The Journal editorial board will send to the first-named author a copy of the Journal offprint.

OBAVEŠTENJE AUTORIMA

Časopis MVM objavljuje orginalne radove koji nisu prethodno objavljivani u drugim časopisima, što je odgovornost autora. Za rad koji je prihvaćen za štampu, prava umnožavanja pripadaju izdavaču.

Časopis se izdaje na engleskom jeziku.

Časopis ***Mobility & Vehicles Mechanics*** se nalazi na SSCI listi.

Svi prispeli radovi se recenziraju. Sva komunikacija se obavlja sa prvim autorom.

UPUTSTVO AUTORIMA ZA TEHNIČKU PRIPREMU RADOVA

Rezime je poseban Word dokument, "*First author family name_ABSTRACT.doc*". Za domaće autore je dvojezičan (srpski i engleski). Inostranim autorima rezime se prevodi na srpski jezik. Ovaj dokument treba da sadrži: 1) ime autora, zanimanje i zvanje, adresu prvog autora preko koje se obavlja sva potrebna korespondencija; 2) naslov rada; 3) kratak sažetak, do 100 reči, 4) do 5 ključnih reči.

Rad je poseban fajl, „*First author family name_Paper.doc*" koji sadrži priloge i slike uključene u tekst. Na kraju rada nalazi se spisak literature i eventualno zahvalnost. Numeraciju korišćenih referenci treba navesti u srednjim zagradama i grupisati ih na kraju rada po rastućem redosledu.

Dužina rada: Najviše 16 stranica B5 formata, ne uključujući rezime
Tekst procesor: Microsoft Word
Margine: levo/desno: mirror margine; unurašnja: 2.5 cm; spoljna: 2 cm, gore: 2.5 cm, dole: 2 cm
Font: Times New Roman, 10 pt
Naslov rada: Velika slova, bold, 11 pt
Naslov poglavlja: Velika slova, bold, 10 pt
Naslov potpoglavlja: Mala slova, bold, 10 pt
Širina tabela,dijagrama: max 125 mm
Nazivi slika, tabela: Figure __ (Table _): Times New Roman, italic 10 pt

Dostavljanje rada elektronski na E-mail: **mvm@kg.ac.rs ; lukicj@kg.ac.rs**

ili poštom na adresu Časopisa
Redakcija časopisa M V M
Fakultet inženjerskih nauka
Sestre Janjić 6, 34000 Kragujevac, Srbija

Po objavljivanju rada, Redakcija časopisa šalje prvom autoru jedan primerak časopisa.

MVM *Editorial Board*
University of Kragujevac
Faculty of Engineering
Sestre Janjić 6, 34000 Kragujevac, Serbia
Tel.: +381/34/335990; Fax: + 381/34/333192
www.mvm.fink.rs